THESIS FOR THE DEGREE OF DOCTOR OF PHILOSOPHY

Ammonia as an Absorbent of Carbon Dioxide in Post-Combustion Capture

- an Experimental, Technical and Economic Process Evaluation

HENRIK JILVERO

Department of Energy and Environment

CHALMERS UNIVERSITY OF TECHNOLOGY

Gothenburg, Sweden 2014

Ammonia as an Absorbent of Carbon Dioxide in Post-Combustion Capture
- an Experimental, Technical and Economic Process Evaluation

Henrik Jilvero
ISBN 978-91-7597-055-4

Doktorsavhandling vid Chalmers Tekniska Högskola
Ny serie nr 3736
ISSN 0346-718X

Department of Energy and Environment
Chalmers University of Technology
SE-412 96 Gothenburg
Sweden
Telephone + 46 (0)31-772 1000

Reproservice
Gothenburg, Sweden 2014

Ammonia as an Absorbent of Carbon Dioxide in Post-Combustion Capture
- an Experimental, Technical and Economic Process Evaluation

HENRIK JILVERO
Division of Energy Technology
Department of Energy and Environment
Chalmers University of Technology

Abstract

Carbon capture and storage is vital to facilitate the transition from our current fossil fuel dependency to a sustainable energy system. The concept of post-combustion capture is based on the selective chemical absorption of carbon dioxide (CO_2). A heat-induced regeneration of the solvent generates the highly concentrated CO_2 stream suitable for storage.

In this work, ammonia is evaluated as an absorbent of CO_2 in post-combustion capture processes. The major goals of this thesis are to define favorable applications and local conditions for ammonia-based post-combustion capture processes. The current benchmarking absorbent, monoethanolamine (MEA), is associated with specific drawbacks, such as a high heat requirement for regeneration and a tendency to undergo degradation during operation. Several novel absorbents, including ammonia, have been proposed as being superior to MEA in these aspects. The major disadvantage of ammonia is its volatility, which results in loss of absorbent (slip).

This thesis reveals the results of experimental, technical and economic performance analyses. To evaluate the capture process, validation of thermodynamic models of the NH_3-CO_2-H_2O system is required. These thermodynamic models rely on a comprehensive experimental data on the solid-liquid-gas equilibrium for all operating conditions. This work presents new gas-liquid equilibrium data for temperatures that are relevant to the absorber (<25°C), which is an operating range of no prior industrial interest. This work presents the results of simulations of the absorption, desorption and ammonia control processes, for both the individual component level and the aggregated capture cycle. The performance of ammonia-based post-combustion capture is evaluated under various operational and local conditions. The design of a full-scale, ammonia-based capture process is described and the cost of capture is estimated for the present process integrated with a coal-fired power plant. Special attention is focused on the design of the absorber system. In this thesis, a dual absorber with intermediate cooling is proposed as an essential measure to reduce ammonia slip. Preferable operating conditions for the absorber system are defined as: lean and rich CO_2 loadings of 0.25 and 0.50, respectively; and a concentration of ammonia (CO_2-free) of 14.3wt%.

The thesis concludes that ammonia-based absorbents represent a feasible alternative to the first- and second-generation absorbents for post-combustion capture of CO_2. The specific total heat requirement for ammonia-based capture is calculated to be approximately 3,000 kJ/kg CO_2. The most serious problem identified with respect to the ammonia process is the cost of reducing the ammonia slip to allowable levels. This concern limits the locations at which the present process could be implemented with commercial success. Successful application of ammonia-based post-combustion capture is expected to be achieved at locations that are characterized by access to low-temperature cooling water (~5°C) and a high concentration of CO_2 (~15vol%).

Keywords: *ammonia, carbon dioxide, carbon capture, process simulations, power plant, cost of capture*

List of Publications

The thesis consists of the following papers:

I. Jilvero, H., Jens, K.-J., Normann, F., Andersson, K., Halstensen, M., Eimer, D., Johnsson, F., *Equilibrium measurements of the NH_3-CO_2-H_2O system. Part 2: Measurement and evaluation of VLE data at low temperatures.* Submitted to Fluid Phase Equilibria, **2014**.

II. Jilvero, H., Normann, F., Andersson, K., Johnsson, F., *The rate of CO_2 absorption in ammonia – implications on absorber design*. Industrial & Engineering Chemistry Research, **2014**.

III. Jilvero, H., Normann, F., Andersson, K., Johnsson, F., *Heat requirement for regeneration of aqueous ammonia in post-combustion carbon dioxide capture*. International Journal of Greenhouse Gas Control, **2012**, *11*, 181-187.

IV. Jilvero, H., Normann, F., Andersson, K., Johnsson, F., *Ammonia-based post combustion – the techno-economics of controlling ammonia emissions*. Manuscript in preparation, **2014**.

V. Jilvero, H., Eldrup, N.-H., Normann, F., Andersson, K., Johnsson, F., Skagestad, R., *Techno-economic evaluation of an ammonia-based post-combustion process integrated with a state-of-the-art coal-fired power plant*, Submitted to International Journal of Greenhouse Gas Control, **2014**.

Henrik Jilvero is the principal author of all five papers. Dr. Fredrik Normann, Dr. Klas Andersson and Professor Filip Johnsson have contributed with discussions and writing to all the papers. Professor Klaus-Joachim Jens and Professor Dag Eimer of Telemark University College have contributed guidance regarding the operational aspects of the experiments and the writing of Paper I. Dr. Maths Halstensen of Telemark University College contributed the Raman spectra analysis and liquid species quantification described in Paper I. Nils-Henrik Eldrup and Ragnhild Skagestad from Tel-Tek, Porsgrunn performed the economic analyses shown in Paper V. As Paper I is the second part of a two-part setup, the first part is included in the *Appendix* as Paper A.

A. Halstensen, M., Jilvero, H., Jinadasa W., Jens, K.-J., *Equilibrium measurements of the NH_3-CO_2-H_2O system. Part 1: Speciation based on Raman spectroscopy and multivariate modeling*. Submitted to Fluid Phase Equilibria, **2014**.

Acknowledgements

I would like to extend my gratitude to the people who have been involved in the work preceding this thesis. My thanks to my examiner, Professor Filip Johnsson who has, despite his busy schedule answered my many inquires with valuable inputs and encouragement, often way outside of working hours. My gratitude also goes to my main supervisor Associate Professor Klas Andersson, for his very constructive inputs into all aspects of my research, which sometimes involves being the one who had to make the tough decisions. My deepest thanks go to my co-supervisor Assistant Professor Fredrik Normann, for whom the phrase "*This work could not have been done without you*" has never been more deserved.

I also thank all the people who have helped me and made me feel welcome at Telemark University College in Porsgrunn, Norway. Foremost, I would like to thank Professor Klaus-Joachim Jens, who made the stay possible and provided the opportunity for me to use his laboratory. His enthusiasm for chemistry is unmatched and highly contagious. I would also like to thank Associate Professor Maths Halstensen for the interesting and smooth cooperation on Paper I. The administrative personnel at Telemark University College and SiTel deserve thanks for all the help they gave with my accommodation. Special thanks also to Per Morten Hansen who helped me with all laboratory-related issues.

My thanks also go to the Combustion and Carbon Capture Technologies Group for fruitful and fun discussions on research, as well as random topics. Many thanks also to my colleagues at the Division of Energy Technology for the nice working atmosphere and taking my mind off the hardships of research with interesting "fika" and lunch discussions. I would like to give special thanks to my long-time office roommate Daniel Bäckström for all the years of shared fun and failures.

The financial support provided by the Norwegian Research Council and the industrial partners in the KMB project (No. 199905/S60), E.ON Sweden, Preem AB, and Energimyndigheten is gratefully acknowledged. Gunn Iren Müller at Hydro Aluminum is acknowledged for the cooperation in the KMB project and the subsequent paper. Dr. Vincent Collins is also acknowledged for his skillful editing of all five papers and the thesis.

My appreciation also goes to my mother and father for the interest they have shown and the support they have given throughout the years. And to my beloved Linn, thank you for your patience during the making of this thesis - I look forward to a future together. Love you!

August, 2014

Henrik Jilvero

Table of Contents

1. Introduction

Global warming resulting from anthropogenic emissions of greenhouse gases may be the greatest environmental challenge that our society has ever faced. In the IPCCs Fifth Assessment Report (AR5), it is stated that it is *extremely likely* that global warming is caused by human influence, mainly through the combustion of fossil-based fuels, leading to the emission of greenhouse gases, especially carbon dioxide (CO_2) [1].

In 2012, fossil fuels represented 82% of the world's primary energy consumption. Figure 1.1 shows the primary energy consumption levels for oil, gas, and coal in megatons of oil equivalents (Mtoe). Even though the total consumption of fossil fuels has stagnated in the OECD countries, there is a steady increase in the global consumption of fossil fuels, which can be attributed to the developing economies [2]. In the World Energy Outlook 2013 (WEO 2013) [3], three scenarios based on future emission policies are presented: 1) a business-as-usual scenario (Current Policies Scenario); 2) a more stringent scenario (New Policies Scenario); and 3) a very stringent policy scenario (the 450 Scenario). The 450 Scenario implies that the atmospheric carbon dioxide equivalents ($CO_{2,e}$[1]) concentration should not exceed 450 ppm, which gives a 50% chance that the global average temperature increase can be kept to <2°C, as compared with pre-industrial levels. In all of the scenarios, the consumption of fossil fuels is expected to increase between Years 2011 and 2035, except in the 450 Scenario, which entails cuts in coal (-1200 Mtoe) and oil (-500 Mtoe) consumption [3], although the use of gas is still expected to increase by 500 Mtoe.

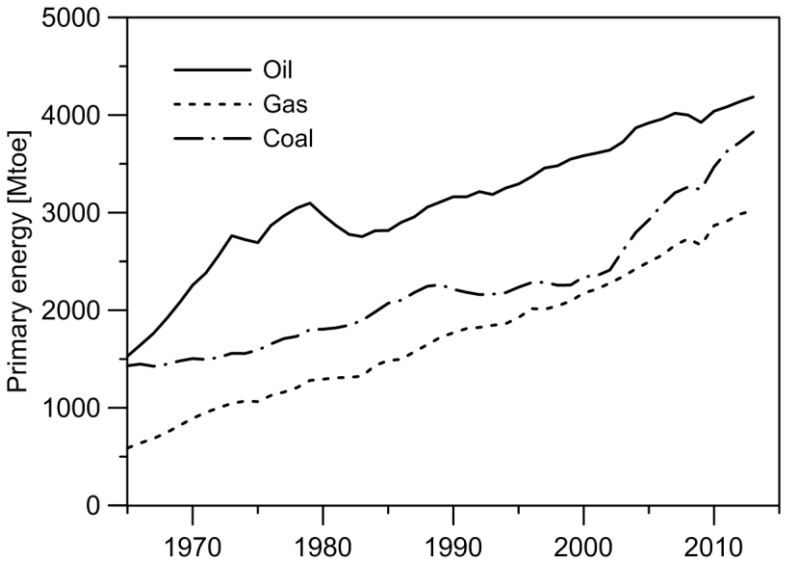

Figure 1.1 Global primary energy consumption (Mtoe) levels of oil, gas, and coal for the period 1965–2013 [2].

An essential measure to reduce CO_2 emission is to introduce a cost for emitting CO_2 to the atmosphere. In Europe, the Emissions Trading Scheme (ETS) has been established, whereby a cap is set for total CO_2 emissions and the market determines the price of emission permits. However, in recent times (2013–2014), this price have been far lower than what is required to push forward extensive investments in CO_2 abatement technologies; allowance prices have been in the range of 3–6 €/tCO_2 [4]. Thus, the estimates made in WEO 2013 for the carbon prices that would be required to

[1] *Includes all greenhouse gases, where the non-carbon dioxide gases are accounted for by their greenhouse effect potential*.

meet the above-mentioned 450 ppm scenario in the ETS system range from 26 to 88 €/tCO_2 over the period 2020–2035, as shown in Figure 1.2 [3].

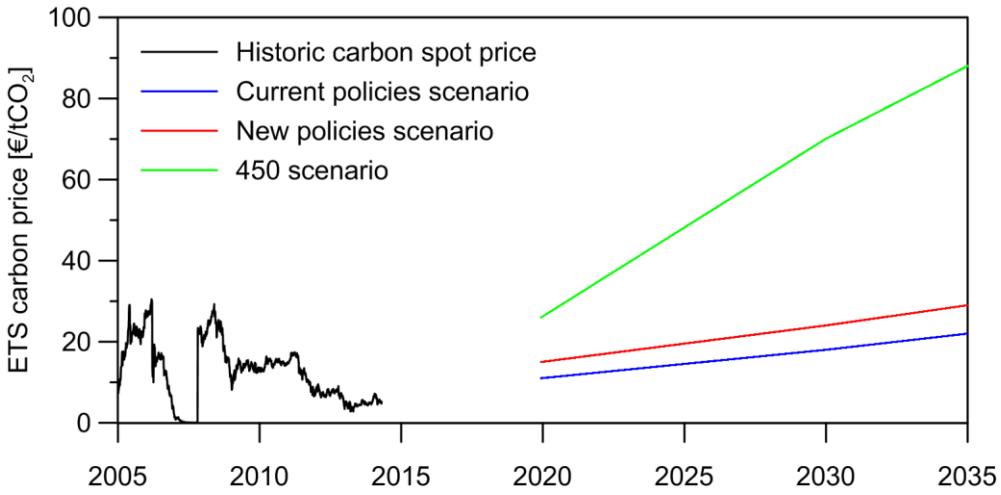

Figure 1.2 The price of ETS CO_2 emission permits both historically [4] and for three future policy scenarios according to WEO 2013 [3]. The prices are converted to $€_{2013}$ from $\$_{2012}$ per tCO_2.

For the 450 Scenario, there is a need for significant cuts in the CO_2 emissions from fossil-based processes. One option to reduce CO_2 levels in the atmosphere is to use carbon capture and storage (CCS). CCS is the only measure that significantly reduces the CO_2 emissions associated with the use of fossil fuels and that prevents the premature decommissioning of existing plants. The alternative to CCS is the deconstruction and phasing out of a large share of the infrastructure of fossil fuel-based processes over a few decades [5]. However, such a reduction in the use of fossil fuel will not be facilitated by the lack of accessible fossil fuels. Large reserves of fossil fuels, especially coal, still remain [2]. Even though the largest share of greenhouse gas emissions is linked to the energy sector (25%), the contribution from the industrial sector is not far behind (21%) [6]. Industrial sectors, such as refining, metallurgy, and cement plants, all consume significant amounts of fossil fuels as integral parts of their respective processes. While carbon-neutral options exist for the energy sector, industrial processes may be associated with inertia in terms of the transition towards allowable emission limits. Rootzén and Johnsson [7] identified the development CCS as a key priority for three key energy-intensive industrial processes (steel, cement, and refining) to meet the emission targets set for industry. The driving force behind CCS is eventually going to be the relationship between the cost of the whole CCS chain (capture, transport, and storage) and the price of CO_2 emission permits. The different policy scenarios (Figure 1.2) will determine when CCS will be required to meet the required reductions in emissions.

The concept underlying CCS is the capture of CO_2 from large point source emitters, e.g., power plants and industries, by separating the CO_2 from the flue gas. The concentrated CO_2 stream is thereafter transported to a suitable geologic storage site. Geologic storage has been employed since 1996 in capturing CO_2 on the Sleipner platform, with subsequent storage in the Utsira formation [8]. Three different "first-generation" capture technologies are usually discussed: post-combustion capture; pre-combustion capture; and oxy-fuel combustion. Whereas the two latter technologies are associated with significant alterations to the original process, post-combustion capture is the most sensible retrofit option, in that it can be applied to an existing plant. This thesis evaluates the prospects of a post-combustion CCS technology. Even though post-combustion capture of CO_2 is a proven technology on the pilot scale, further research on the operation, safety, cost, and optimization of the process will be required before full-scale commercialization can be realized.

1.1. Objectives

The overall objective of the work presented in this thesis is to carry out experimental, technical, and economic evaluations of the performance of ammonia-based, post-combustion capture. Given the variety of CO_2 point sources under different conditions, e.g., flue gas CO_2 concentrations, integration possibilities, and the local environment, knowledge is needed to define the on-site characteristics required for successful implementation of ammonia-based, post-combustion capture. This thesis aims to contribute to the evaluation and development of ammonia-based, post-combustion capture, primarily within the following three areas:

(i) Evaluation of the fundamental framework of the NH_3-CO_2-H_2O system. This involves a review of the existing experimental outcomes and thermodynamic modeling results on the NH_3-CO_2-H_2O system, so as to execute state-of-the-art in thermodynamic modeling of the system. Furthermore, this work generates new experimental phase equilibrium data at temperatures below 25°C, facilitating the generation or validation of thermodynamic models.

(ii) Design and optimization of unit operations within the capture process. This part of the work aims to optimize the operating conditions for ammonia-based, post-combustion capture with respect to the heat requirement, CO_2 capture efficiency, and ammonia slip. Each of the major process units (absorber, stripper, and water wash) are evaluated individually and combined in the ammonia-based, post-combustion capture process.

(iii) Implementation and integration of the capture process. This work aims to estimate the capital expenditures (CAPEX) and operating expenditures (OPEX) of the implementation of the ammonia-based capture process. A prerequisite for this is a detailed process description of a full-scale capture process.

1.2. Outline of the thesis

This thesis is based on five papers (Papers I–V). Paper I represents the second part of a two-part publication; the first part (Paper A) is appended to the thesis. As the methodology presented in Paper A was developed primarily by one of the co-authors, this methodology is not in focus in the present thesis. The thesis starts with the present *Introduction*, which summarizes the appended papers and places the work in a broader perspective. Chapter 1 of the *Introduction* gives the background and the aims of the thesis. Post-combustion capture is introduced in general terms in Chapter 2, and the ammonia-based, post-combustion capture process is outlined specifically in Chapter 3. The overall methodology of the thesis, presented in Chapter 4, includes a validation of the thermodynamic models. The results of the thesis are divided into three chapters. Chapters 5–7 comprise discussions of the operation of the capture process at the technical, process, and economic levels. The *Discussion*, *Conclusions*, and *Suggestions for Future Work* are given in Chapters 8, 9 and 10, respectively. In brief, the appended papers cover the following topics:

Paper I A literature review of the gas- and liquid-phase equilibrium composition data for the NH_3-CO_2-H_2O system reveals a lack of data for the temperature range of the absorber. The equilibrium partial pressures of CO_2 at these temperatures are measured by gas chromatography. The methodology for liquid speciation by Raman spectroscopy, presented in Paper A (Appendix), is employed to elucidate the carbon distribution in the liquid phase. Predictions based on an existing thermodynamic model are compared with the experimental data.

Paper II The reaction rate of absorption of CO_2 to aqueous ammonia is addressed. A rate-based simulation approach is used to establish a predictive model of the absorption column. The absorber model is validated against experimental pilot plant data. The performances of different absorber designs are evaluated. The operating conditions and the design of the absorber are presented.

Paper III Equilibrium-based process simulations is used to model the behavior of the carbon capture process of ammonia-based post-combustion capture of CO_2. The paper evaluates the heat requirement at different process conditions. Operating conditions are suggested where the heat requirement is minimized.

Paper IV The slip of ammonia from the capture process is a major problem associated with the ammonia-based CO_2 capture process. This paper explains the primary operational measures that can be used to reduce ammonia slip. Three different ammonia control designs are evaluated with respect to reduction potential, energy penalty, and cost. Paper IV suggests a suitable strategy for ammonia control and defines the site-specific conditions that are advantageous for ammonia control.

Paper V The conclusions from the Papers I–IV are implemented into the design of a full-scale, ammonia-based capture process. A detailed process description of a full-scale ammonia-based capture process is presented. The capture process is integrated with a coal-fired power plant. Based on a detailed equipment list, the CAPEX and OPEX values of the ammonia process are calculated.

2. Post-Combustion Carbon Dioxide Capture

2.1. Process design

Absorption of acid gases has been utilized for many decades - the first patent of an industrial process dates back to the 1930's [9]. At that time, the purpose was to increase the purity of natural gas by absorbing acid gases, such as CO_2 and H_2S. The general setup of the absorption process has remained the same and includes two columns, one in which CO_2 is absorbed by the liquid solvent (absorber), and one in which CO_2 is released (stripper). The driving force for the separation between the two columns is a temperature and/or pressure difference. The absorber, stripper, and a heat exchanger placed in between make up the essential units of a post-combustion capture process. A schematic of a generic post-combustion capture process is presented in Figure 2.1. The flue gas stream (stream A in Figure 2.1) enters the bottom of the absorber column (unit 1 in Figure 2.1). At the top of the absorber, a liquid (Stream C) is distributed over a packing material, flowing countercurrent to the flue gases. The liquid consists of an absorbent that selectively absorbs CO_2. The absorbent is usually diluted with water. The absorption reaction is exothermal, so there is a temperature increase in the reactive parts of the column. A common design target is to, within the absorber capture 90% of the CO_2 in the flue gases [10]. Other gaseous species, such as nitrogen in the case of flue gas cleaning, are expected to be inert within the absorber.

The liquid stream that enters the top of the absorber is referred to as the CO_2-lean stream (Stream C) because it contains a small amount of CO_2 and has the capacity to absorb more CO_2. The liquid stream that exits the bottom of the absorber is called the CO_2-rich stream (Stream D). The amount of CO_2 that is captured is represented by the CO_2-loading (mole CO_2/mole absorbent) in the liquid phase. The commonly used terminology for post-combustion capture is given in Table 2.1. A concept that is introduced in Paper II is that of *Absorber loading*, which describes the mole-ratio of the absorbent in the lean stream to the CO_2 in the flue gas stream. More commonly, the relationship between the liquid (L) and gas (G) flow rates (L/G-ratio) is calculated. However, this relationship is linked mainly to the flows through the column. Absorber loading becomes an important design parameter for evaluating the reactive process in the absorber.

Table 2.1 Nomenclature for the design parameters used in post-combustion capture. The stream notation corresponds to that shown in Figure 2.1

Variable	Definition	Unit
Lean-CO_2 loading	$\dot{n}_{CO_2}/\dot{n}_{NH_3}$ (Stream C)	-
Rich-CO_2 loading	$\dot{n}_{CO_2}/\dot{n}_{NH_3}$ (Stream D)	-
CO_2 capture efficiency	$\dot{n}_{CO_2}$ Stream E/$\dot{n}_{CO_2}$ Stream A	[%]
Ammonia slip	$\dot{n}_{NH_3}$ Stream B/$\dot{n}_{tot}$ Stream A	[ppm]
Absorber loading	$\dot{n}_{CO_2}$ Stream C/$\dot{n}_{NH_3}$ Stream A	-
Heat requirement for regeneration	$Q_{reboiler}/\dot{m}_{CO_2}$ Stream E	[kJ/kg CO_2]
Heat requirement for ammonia stripping	$Q_{NH3,\ stripper}/\dot{m}_{CO_2}$ Stream E	[kJ/kg CO_2]

The CO_2-rich stream that exits the absorber is transported to the rich/lean heat exchanger (Unit 2), where the stream is heated. In the stripper column (Unit 3), heat is added to a reboiler, in which the absorption reactions are reversed. This heat is supplied in the form of a process steam (Stream F). One of the most important performance indicators of post-combustion capture is the amount of heat (kJ_{th}) that is required to release a certain amount of CO_2 (kg CO_2 captured). This parameter is referred to as the specific heat requirement of regeneration or the specific reboiler duty (kJ/kg CO_2). The outlet streams from the stripper are: the liquid CO_2 lean stream that exits the bottom of the stripper; and the gaseous stream of concentrated CO_2 that is discharged from the top of the stripper. Heat from the lean stream is retaining by heat exchange with the rich stream, thereby closing the loop. The CO_2 stream is purified by condensing the residual water and absorbent. To be suitable for transport *via* a pipeline, the CO_2 needs to be in a supercritical state (Stream E). This means that the pressure has to be >70 bar at room temperature. The pressurization of the CO_2 is carried out in several stages with intermediate intercooling (Unit 4).

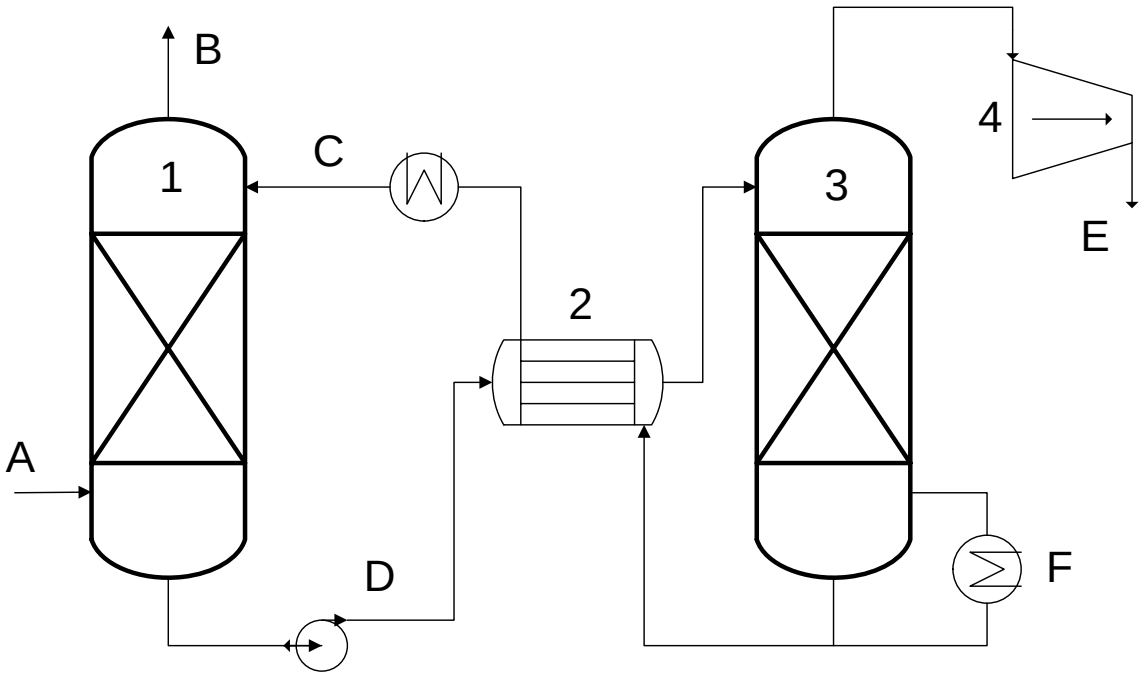

Figure 2.1 Schematic of a generic post-combustion CO_2 capture process. 1, Absorber; 2, rich/lean heat exchanger; 3, stripper; 4, CO_2 compression; A, flue gas stream; B, gas to stack; C, process steam; D, compressed CO_2.

2.2. Absorbents

Either a physical or a chemical absorbent can be used for post-combustion capture of CO_2. In contrast to chemical absorbents, physical absorbents are non-reactive and rely solely on the solubility of the gas in the liquid. In chemical absorption, the CO_2 reacts with the absorbent and forms a weakly bonded compound in a process that can easily be reversed by applying heat. This thesis focuses on chemical absorption. The development of absorbents is one of the most important areas of research into the performance of post-combustion capture processes. Absorbents are evaluated with respect to a number of performance indicators, the most important of which are:

- Absorption kinetics
- Heat requirement for regeneration
- Persistence to degradation
- CO_2-loading capacity
- Corrosiveness
- Volatility
- Price
- Toxicity
- Ease of operation

It should be noted in order to be considered as interesting, all candidate absorbents must fulfill to some extent all the above criteria. The most well-established absorbents include alkanolamines, sterically hindered amines, and piperazine.

Primary, secondary and tertiary alkanolamines

The absorbents that are most commonly used in post-combustion capture are alkanolamine-based, with the most frequently reported being primary (monoethanolamine; MEA), secondary (diethanolamine; DEA) and tertiary (triethanolamine; TEA) amines. These compounds differ with respect to the number of hydroxyl groups per amino group (see below for the molecular structures). In the primary amines, there is one hydroxyl group per amino group, whereas in the tertiary amines, there are three hydroxyl groups per amino group. In the case of the tertiary amine methyl diethanolamine (MDEA), one of the hydroxyl groups is replaced by a methyl group. Primary amines are generally more alkaline. In general, primary and secondary amines have faster reaction rates but suffer from a high heat requirement for regeneration, as compared with tertiary amines. An important area of research is to investigate combinations of different types of amines with positive synergies and optimal properties. For example, tertiary alkanolamines can be mixed with primary and secondary alkanolamines to reduce the heat requirement for regeneration.

MEA has for a long time been considered as the benchmarking absorbent for post-combustion capture. Thus, it is the absorbent with which other absorbents are compared. The ability of MEA to capture CO_2 at low partial pressures and its reliable operation have made it the absorbent of choice for many current industrial applications (e.g., the removal of CO_2 from natural gas and synthesis gases). Other advantages are a relatively low molecular weight, high alkalinity, and a long experience with its application [11]. However, the MEA process has inherent disadvantages, in that it has a tendency to degrade during operation, especially in oxidative environments; and it has a relatively high heat requirement for regeneration. Depending on the process conditions, the heat requirement can be 3,200–5,000 MJ/kg CO_2 [10]. The MEA concentration is usually 30 wt%, and the CO_2 loading ranges from 0.21 to 0.47. The absorber is operated under atmospheric conditions and at around 40°C, with a temperature profile that peaks at 80°C. The stripper conditions are restricted to 2.2 bar at 130°C, to avoid degradation.

Sterically hindered amines

Another group of amines comprises the sterically hindered amines. One example is the sterically hindered version of MEA, 2-amin-2-methyl-1-propanol (AMP). The sterical hindrance of the amino group prohibits the formation of a stable carbamate, as occurs in the cases of primary and secondary amines. The formation of an unstable carbamate allows subsequent formation of bicarbonate, which can carry one mole of CO_2 per mole of amine, as compared to carbamate, which only carries one mole

of CO_2 per two moles of amine. This means that sterically hindered amines are associated with lower heat requirement for regeneration and lower equipment costs, whereas they do not have the poor reaction rates of tertiary amines. Proprietary absorbents, such as KS-1 produced by Mitsubishi [12], are based on sterically hindered amines. The performance data for these absorbents are sparse, although a heat requirement of 2,600 kJ/kg CO_2 and loading capacities higher than that of MEA have been claimed [12].

Piperazine

An absorbent that recently has received a lot of attention and that may offer several advantages is piperazine (PZ). PZ is a diamine with capacity to absorb 2 moles of CO_2 per mole of PZ. The advantages of PZ are a low heat requirement (2,600 MJ/kg CO_2, according to simulations), a much faster absorption rate, less degradation, less corrosion, and lower volatility [13]. However, the chemistry of the PZ solution is more complex than that of other amine-based processes because zwitterions and precipitation are required to describe the PZ-CO_2-H_2O system. The process is operated with 40wt% PZ solution and an absorber temperature of 40°C. A disadvantage is that the operating range of the CO_2 loading is narrow (0.31–0.41 mol/2·mol PZ), so as to avoid precipitation. The complex chemistry of PZ also demands a more complex process design. The regeneration process is divided into a high-temperature, two-flash system at two pressure levels. Pilot plants that use PZ are uncommon. The University of Texas at Austin has successfully operated a 0.1-MW pilot plant with the two-flash regeneration system [14]; the heat requirement was 3,230 MJ/kg CO_2.

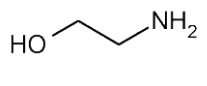

Monoethanolamine (MEA)

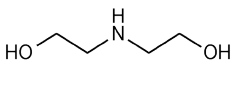

Diethanolamine (DEA)

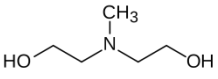

Methyl diethanolamine (MDEA)

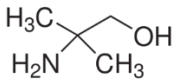

2-Amino-2-methyl-1-propanol (AMP)

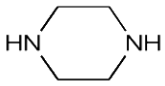

Piperazine (PZ)

Amine degradation

As mentioned above, amines have a tendency to undergo degradation during operation. This means that the absorbent has to be continuously replaced and the used absorbent has to be dispatched. There are three main reaction routes for MEA. 1) thermal degradation; 2) oxidative degradation; and 3) carbamate polymerization [15]. Thermal degradation becomes increasingly important at temperatures >130°C. Oxidative degradation is more important as it involves reactions with the oxygen in the flue gas, as well as impurities, such as SO_x and NO_x. Since MEA is very sensitive to SO_x and NO_x, these pollutants must be removed before entry into the absorber, with the concentration of SO_x ideally being <10 ppm [16]. Some degradation products are particularly dangerous (carcinogenic), e.g., the nitrosamines, which are formed through oxidative degradation through reactions with NO_2 and amines. The levels of nitrosamines need to be controlled before the gas from the absorber can be released to the atmosphere [17]. The consumption of MEA due to degradation can be as high as 3.6 kg MEA/tCO_2 captured [18]. To remove the degradation product, a slipstream from the process is directed to a reclaimer, where heat is applied to remove non-volatile products. The non-volatile part of the slipstream is dispatched as reclaimer waste. Absorbents with very low partial pressures are not easily evaporated in the reclaimer. The most common reclaimer waste handling procedure is incineration. Efforts have been made to find alternatives for the reclaimer waste disposal, such as biological degradation [19], incineration, and application as a NOx-reducing agent *via* selective non-catalytic reduction (SNCR) [20]. The cost of amine loss is expected to be less than 5 \$/tCO_2 (not

including waste handling) [10]. The loss of absorbent is, however, not the only problem associated with amine degradation. The degradation products can cause other problems, such as foaming, fouling, plugging, increased viscosity, and perhaps the most problematic, increased corrosion. The rate of degradation is even catalyzed by corrosion products (metal ions) [21]. Figure 2.2 shows the rates of development of degradation products and metals in the solvent over time, as reported by Reider and Unterberger [21]. The figure shows that the rate of degradation increases in the presence of corrosion products. While the amine-based absorbent performs well with respect to most of the criteria, the problem of degradation persists. Efforts have been made to identify absorbents that are less prone to degradation, e.g., potassium carbonate and ammonia, with the latter being in focus in the present work.

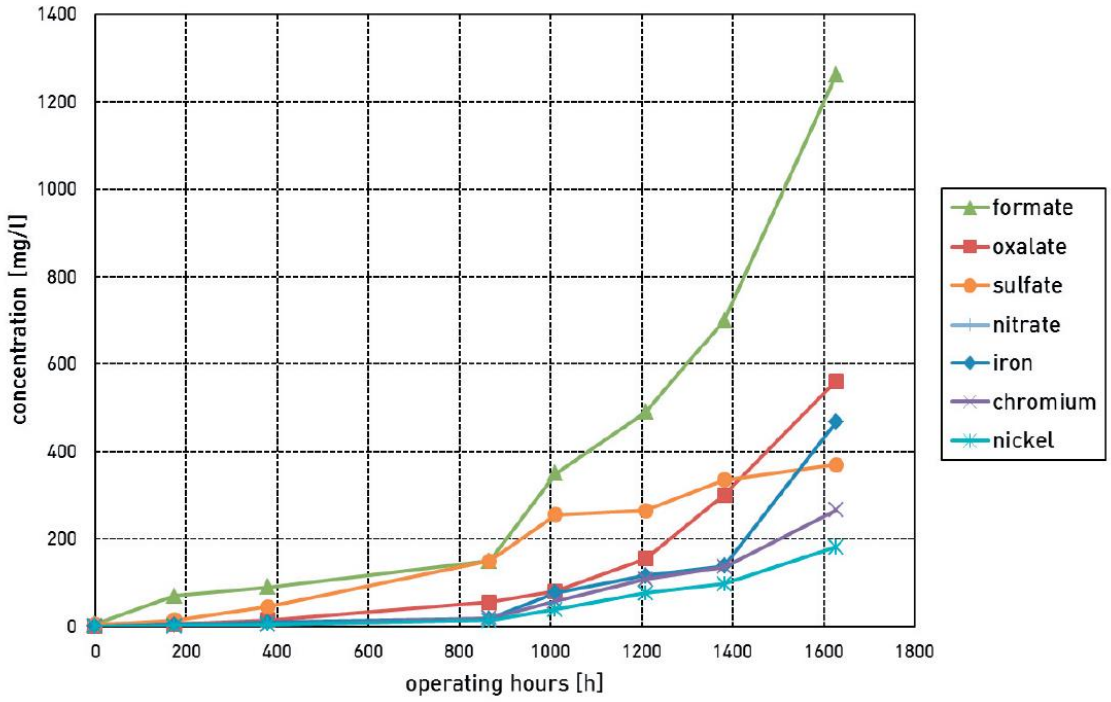

Figure 2.2 Development of degradation products and metals during a measurement campaign. Source: Reider and Unterberger [21].

3. Ammonia as Absorbent of Carbon Dioxide

Ammonia has emerged as a plausible alternative absorbent of CO_2 in post-combustion capture. The aim of this chapter is to introduce the theory of CO_2 absorption into aqueous ammonia, as well as to outline previous work performed in the field of ammonia-based, post-combustion capture. The outcomes of the previous studies include experimental, process simulation, and pilot plant results. Much work has been conducted on the NH_3-CO_2-H_2O system over the years. Both experimental equilibrium phase composition data and reaction kinetics data are important for this work. These data are used as the basis for thermodynamic modeling and for process simulations of ammonia-based, post-combustion capture. Developing thermodynamic models of the equilibrium behavior of the NH_3-CO_2-H_2O system has been ongoing for many decades. These models have been used extensively in simulation studies of the capture process. In the past 8 years, at least nine different pilot plants with thermal capacities in the range of 0.025–54 MW_{th} have been employed to demonstrate the operation of ammonia-based, post-combustion capture.

In 1997, the group of Bai et al. [22] was one of the first to propose ammonia as an absorbent of flue gas CO_2. They discovered that ammonia has a high capture capacity, up to 1 kg CO_2/kg NH_3. However, it was also noted that the high volatility of ammonia could be a major issue. Since the publication of the paper of Bai et al. [22], different processes with ammonia as the absorbent of CO_2 have been proposed, including the chilled ammonia process, the ECO2 process, and the aqueous ammonia process.

Chilled ammonia process

It was not until 2006, when the "Chilled ammonia process" (CAP) was patented [23], that ammonia-based, post-combustion capture started to receive attention. The CAP was proposed to have several advantages over the amine-based processes, including a significantly lower heat requirement for regeneration, less degradation, and a higher CO_2 loading capacity [24]. An important feature of the initial concept of the CAP was that precipitation was expected to occur in the low-temperature stage of the process. Thus, a slurry is formed, which has consequences for the process design. Due to slurry formation during the absorption, the absorber is a combination of an open spray tower and a flooded tray. To reduce ammonia slip and increase the capture capacity, absorption should occur at low temperatures (0°–20°C). These low absorber temperatures are achieved through refrigeration. The rich stream contains 10%–15% crystals; using a hydrocyclone, the solid content can be increased to 50%–60%. Then, a slurry pump is used to increase the pressure of the slurry to 20–40 bar. The stripper is operated at the same pressure and in the temperature range of 100°–150°C [24]. The company Alstom has been leading the development of the CAP. As presented in Figure 3.2, pilot plants have been commissioned since Year 2006, and the process has been developed in the intervening period. As the original version of the CAP proved to be operationally problematic, there has been a gradual shift of the CAP toward the operational conditions of the aqueous ammonia process, i.e., without precipitation. The most recent pilot plant is the 40-MW_{th} pilot plant based at Mongstad [25].

ECO2

The proprietary process ECO2 (Powerspan) has been developed since 2004 in cooperation with the U.S. Department of Energy (DOE) National Energy Technology Laboratory (NETL) [26]. The process is based on principles similar to those of the CAP. However, they propose a multi-pollutant control

system in which SO_x and NO_x reduction is also possible. In a pre-treatment unit located upsteam the absorber, ammonia is used to capture both SO_x and NO_x simultaneously. A 1-MW_{th} pilot plant at FirstEnergys's R.E. Berger Plant was constructed in Year 2008 to evaluate the process. An independent assessment of the ECO2 process revealed a heat requirement of 1000 Btu/lb CO_2 (2326 kJ/kg CO_2) [27]. There were early plans for two demonstration plants with capacities of up to 120 MW, where the CO_2 was going to be used for enhanced oil recovery (EOR). Although both plants were scheduled to enter operation in Year 2012, the plan either got canceled or was shifted to another capture technology [28].

Aqueous ammonia process

Another configuration of ammonia-based, post-combustion capture is the aqueous ammonia process (AAP). Figure 3.1 shows a schematic of an AAP capture facility. The initial process description by Bai et al. [22] is similar to the AAP. The AAP will be the process configuration in focus in this thesis. The operating conditions and process design of AAP differ somewhat from the CAP. The major differences are that precipitation is not allowed to occur, and that the water concentration is higher. Precipitation is alleviated primarily through a decreased concentration of ammonia, which means that more water is added. The AAP operates at an ammonia concentration in the range of 5–15 wt%, whereas the CAP operates at 28wt% [29]. The lack of solids allows for a more typical absorber design, i.e., a packed column. Another difference is that the absorber operating temperature is as low as the available cooling media allows, so refrigeration is not used. The AAP may entail a higher cost for equipment due to the extra water, as well as a higher heat requirement than the CAP. However, the absence of slurry handling makes the process much easier to operate. The AAP process has been demonstrated at the pilot plant scale by Yu et al. [30], wherein a low concentration of ammonia (5 wt%) was used.

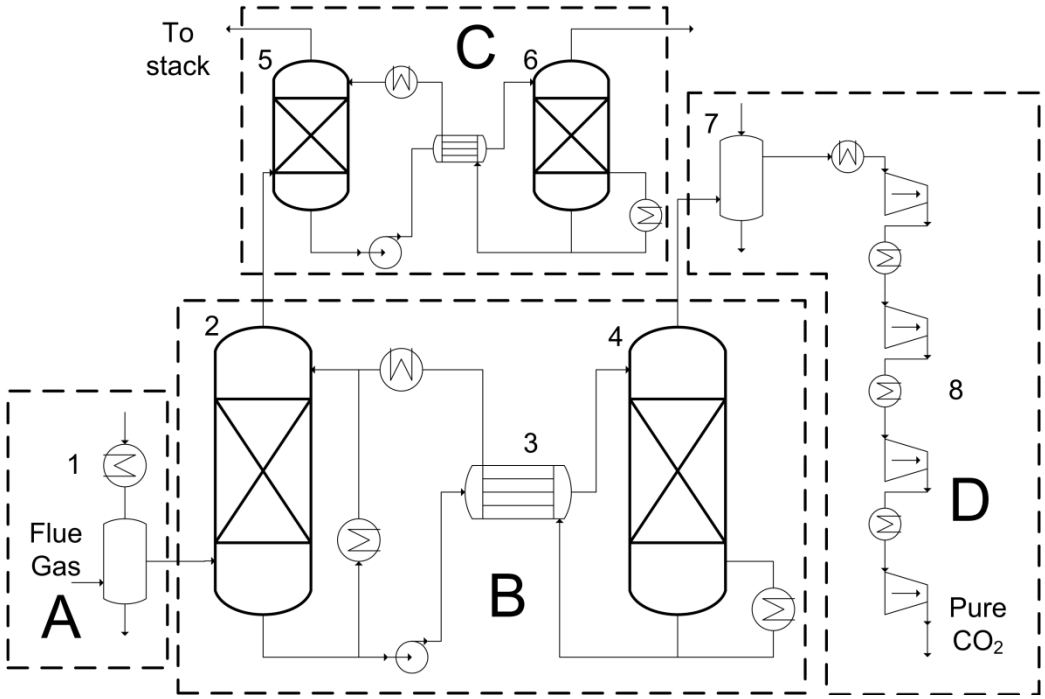

Figure 3.1 Detailed schematic of an ammonia-based, post-combustion process. A, Flue gas conditioning and cooling system; B, CO_2 capture cycle; C, ammonia abatement cycle; D, CO_2 compression. 1. Flue gas conditioning; 2, absorber; 3, rich/lean heat exchanger; 4, stripper; 5, water wash; 6, ammonia stripper; 7, CO_2 wash; 8, multi-stage compression.

Ammonia emission control methods

The high volatility of ammonia means that the stream that exits the top of the absorber may contain a significant amount of ammonia. This ammonia is referred to as slip. A common design limitation for ammonia emissions is that the discharge concentration of ammonia in the stack may not exceed 10 ppm. The ammonia emission limits may vary between different countries and may even be site-specific. However, the limits are always close to 10 ppm. The National Institute for Occupational Safety and Health (NIOSH) has listed 25 ppm as the time-weighted average limit for 8-hour exposure intervals.

The most common method to control the emission of ammonia is to use a so-called "ammonia abatement cycle" (Process C in Figure 3.1). The emission of ammonia is reduced with a water wash (Unit 5 in Figure 3.1) before discharge. The ammonia-containing solution is regenerated to recover most of the ammonia to the CO_2 capture cycle (Unit 6). Different primary and secondary methods to reduce the problem of ammonia slip are evaluated in Paper IV. The ammonia abatement cycle is the most commonly proposed ammonia recovery method. The ammonia is captured in a water wash, and the captured ammonia is directed to an ammonia stripper where heat (steam) is applied to concentrate the ammonia in the gas phase. This method is regenerative, as the ammonia can be re-introduced into the process. The primary operating cost of ammonia abatement cycle is the cost of process steam. Other ammonia control methods that are evaluated in Paper IV are staged absorption, chilled absorption and acid washing. The chilled absorption option is a primary ammonia recovery method, in which the partial pressure of ammonia is reduced by decreasing the operating temperature of the absorber. Process chilling is used to reduce the operating temperature (5°C). This process requires electricity. When the acid wash option is applied the water in the water wash is replaced with dilute acid (e.g., sulfuric acid). The acid reduces the pH-level, thereby enhancing ammonia absorption. A commercial by-product is formed, although both ammonia and sulfuric acid are consumed in the process.

3.1. Previous work on ammonia-based post-combustion

Pilot plants

Since 2006, a considerable amount of work has performed on ammonia-based, post-combustion capture, including the construction of nine pilot-scale plants (see Figure 3.2). The company Alstom has been pushing the development of the CAP and is responsible for five of the pilot plants that have entered operation. The company Powerspan has also demonstrated their ECO2 process on a pilot scale [26]. Other organizations that have evaluated ammonia-based post-combustion in pilot-scale plants are the Research Institute of Industrial Science and Technology (RIST) in Korea [31] and the Commonwealth Scientific and Industrial Research Organization (CSIRO) in Australia [30]. Many of the planned demonstration-scale plants have been canceled due to unclear forward-looking policies with respect to emissions targets or due to lack of funding [28]. Although the cancellations have not been confined to ammonia-based post-combustion, many of the planned CCS-related projects have been canceled. The only pilot plant that is currently operating is the 40-MW_{th} plant located at Mongstad TCM [25]. The most comprehensive operational results for ammonia-based post-combustion come from the work conducted by CSIRO, published by Yu et al. [30]. The experimentally determined CO_2 capture efficiency along the height of the absorber is used for the model validation in Paper II. In their pilot plant, they also used a pre-treatment unit in an attempt to capture SO_x and NO_x. The results showed an almost 95% reduction in SOx levels but no measureable reduction of NO_x levels.

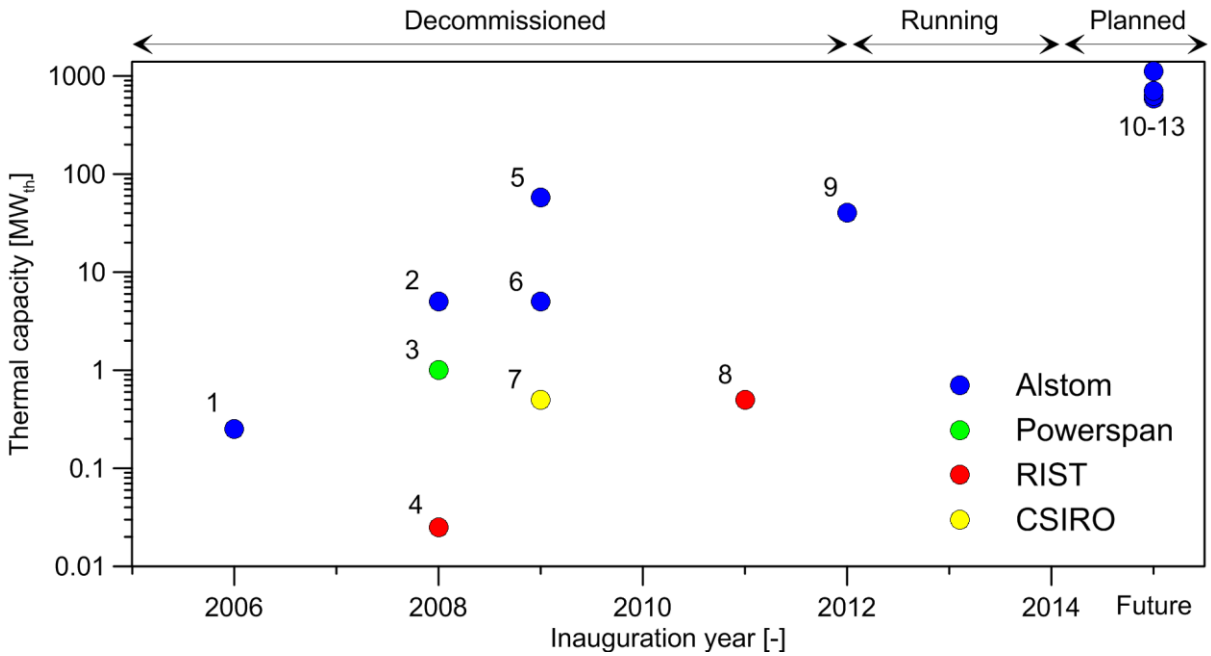

Figure 3.2 Overview of pilot plants and planned demonstration plants using ammonia as the absorbent. The colors of the symbols indicate the responsible supplier or organization. Location/Project: 1, Växjö; 2, Pleasant Prairie; 3, Berger; 4, Pohang Steel Works; 5, AEP Mountaineer; 6, Karlshamn; 7, Munmorah; 8, Pohang Steel Works; 9, Mongstad TCM; 10. AEP Mountaineer (canceled); 11, Transalta (canceled); 12, Getica – CET Turceni (?); 13, Mongstad CCM (canceled). (Assumptions are made where only the flue gas flow rate or electric capacity is given)

Process simulations

Process simulations of ammonia-based post-combustion have been performed by a number of research groups [32-34]. Several studies have evaluated the specific heat requirement of ammonia regeneration, with large discrepancies between sources, as shown in Figure 3.3. Paper III discusses these discrepancies. As a reference, the corresponding heat requirement of MEA regeneration is 3,200–5,000 kJ/kg CO_2 captured (mostly around 3,700 kJ/kg CO_2). In Figure 3.3, the methodologies that have been used in the studies are indicated. The early publications [24, 26, 35] estimated that the heat requirement was governed by the reaction between ammonium carbonate and ammonium bicarbonate (R1). This is an important feature of the CAP, which, if achievable, would entail a low heat requirement in the range of 1,000–1,500 kJ/kg CO_2.

$$2NH_4^+ + CO_3^{2-} + CO_2(g) + H_2O \rightleftharpoons 2NH_4^+ + 2HCO_3^- \qquad \Delta H = 26.88\ kJ/mol \qquad \text{(R1)}$$

Most of the process simulation estimates has been performed with an equilibrium-controlled absorption in Aspen Plus. Paper III, which is also included in Figure 3.3, shows that it is not possible to run the process according to reaction R1. The equilibrium-based simulations result in a heat requirement for ammonia regeneration in the range of 2,000–3,000 kJ/kg CO_2. In recent years, rate-based simulations of the absorption have been performed. These simulations indicate a heat requirement >3,000 kJ/kg CO_2. In the study conducted by Zhang and Guo [34], they have developed a rate-based model for the pilot plant data from the Munmorah pilot plant [30]. The pilot plant operation reported a heat requirement of 4,000–4,200 kJ/kg CO_2, while the simulation showed a heat requirement of 3,630 kJ/kg CO_2. However, as mentioned in Paper III, the pilot plant operating conditions were not ideal with respect to heat requirement. A more-optimized process with respect to heat requirement is presented in Paper V, with the results showing a heat requirement of 3,060 kJ/kg CO_2.

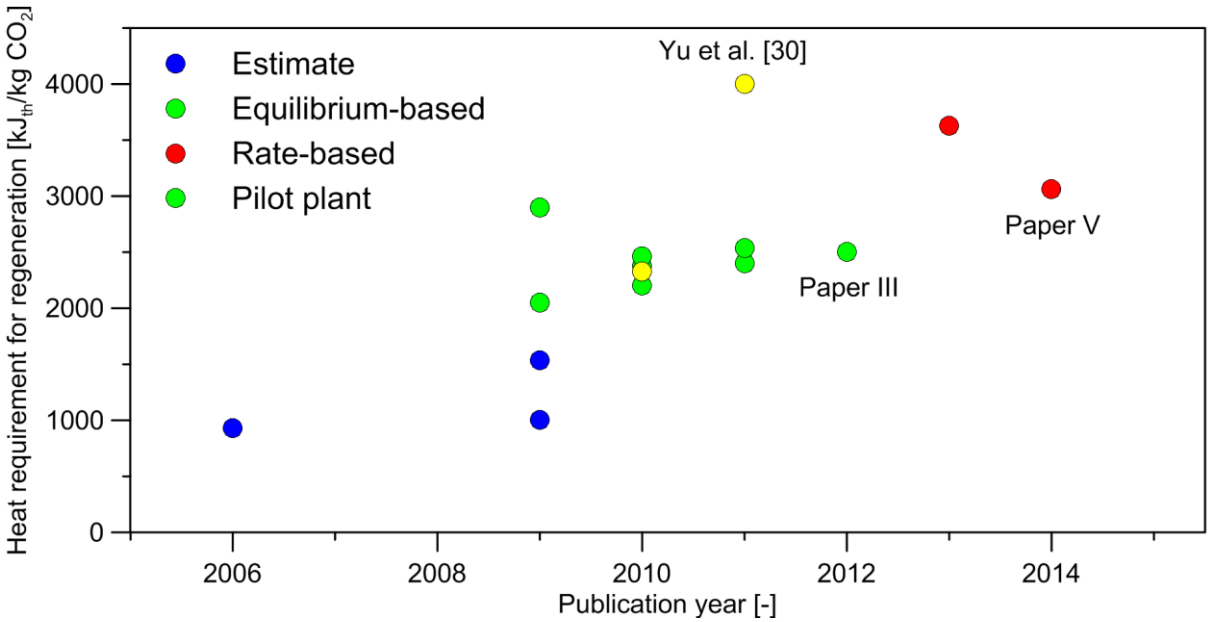

Figure 3.3 Data from the literature on the heat requirement for regeneration. The sources according to the evaluation method used: Estimate [24, 26, 35]; Equilibrium-based [29, 32, 36-40]; Rate-based [34]; Pilot plant [27, 30]. (In the Estimate case, the overall process is estimated to be governed by the reaction between ammonium carbonate and ammonium bicarbonate, i.e., reaction R1)

Process integration and economic estimations

The ammonia-based post-combustion carbon capture process may be applied to any type of CO_2 emission source. Most process integration studies have been performed on power plants. Table 3.1 presents the results and economic assumptions made in studies of ammonia-based, post-combustion of CO_2 integrated with power plants. The power plant efficiency decrease reported in most of the studies is in the range of 8.4%–9.2%. Two separate studies has estimated the cost of capture at 39.2 $€_{2013}/tCO_2$ [33] and 60.2 $€_{2013}/tCO_2$ [41]. The economic assumptions and results from Paper V are also included in Table 3.1. Studies on capture from industrial process with the AAP are sparse. However, the aim of much of the work performed at RIST [31] has been integration with the iron-making industry, and an upcoming study (not included in this thesis) will investigate integration with the aluminum [42] and refining [43] industries.

Table 3.1 Studies in which ammonia-based, post-combustion capture of CO_2 has been implemented with a power plant.

Source	Jilvero et al. [38]	Linnenberg et al. [44]	Versteeg and Rubin [41]	Valenti et al. [33]	Paper V
Capture technology	CAP	AAP	CAP	AAP	AAP
Absorber modeling approach	Eq.-based	Eq.-based	Eq.-based	Eq.-based	Rate-based
Efficiency decrease [LHV %]	9.2 %	8.5 %	11.2 %[1]	8.4 %	9.2%
Annual load factor [h]	-	-	6570	7500	8000
Interest rate [%]	-	-	8.25	8	7.5
Economic life-time [years]	-	-	30	40	25
Capture cost [€$_{2013}$/tCO$_2$]	-	-	60.2[2]	39.2[3]	35.0

[1] Higher heating value

[2] Converted from 73.2 $\$_{2007}$

[3] Converted from 38.6 $€_{2012}$

3.2. Chemistry of the NH_3-CO_2-H_2O system

The mixture of CO_2 and aqueous ammonia forms a complex, weak electrolyte. Figure 3.4 shows an overview of the chemistry of the NH_3-CO_2-H_2O system for the gas, liquid and solid phases. The gas phase is assumed to be non-reactive, and only the vapor-liquid equilibrium (VLE) of ammonia, CO_2, and water is considered. As the liquid solution is a weak electrolyte, it includes both molecular and ionic species. The molecular species will dissociate to ions. Within the scope of this thesis, only one solid species is considered (ammonium bicarbonate; $NH_4HCO_3(s)$). Under conditions not considered in this work, other solid species may form. In this thesis, different approaches are used to represent the chemistry. When considering different absorption routes, i.e., which species the CO_2 is bound to in the liquid, it can prove useful to look at the global reaction mechanisms. Thus, to identify the reactions between gaseous carbon and aqueous ammonia, which form the ionic products carbonate (CO_3^{2-}), bicarbonate (HCO_3^-), and carbamate (NH_2COO^-). This will give an indication of the enthalpy change of the different absorption routes, and thereby the heat of absorption. However, in the modeling of the NH_3-CO_2-H_2O system, there are two approaches: equilibrium-based and rate-based. The equilibrium-based approach is based on a set of reactions that dictate the degree of dissociation and thus, the liquid composition. In the rate-based approach, some of the CO_2 absorption reactions account for the reaction kinetics. Both the equilibrium-based and rate-based approaches require an experimental basis. The experimental backgrounds of these two approaches are presented in Chapter 3.3.

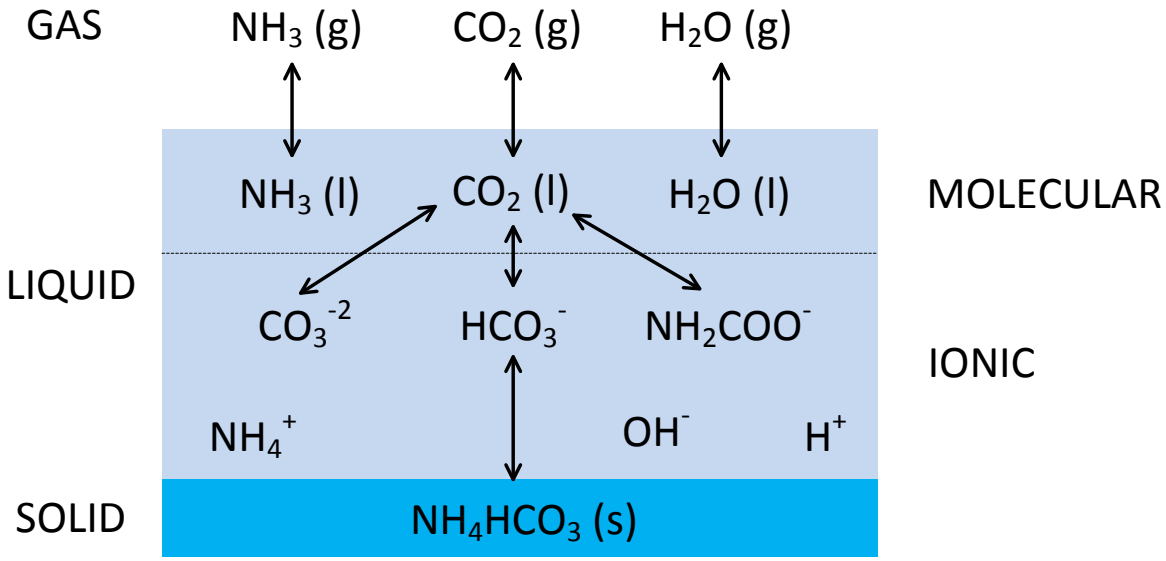

Figure 3.4 Schematic of the chemistry of the NH_3-CO_2-H_2O system, including designations of the species in the vapor, liquid and solid phases.

Global reactions

In an aqueous ammonia solution, gaseous CO_2 may be absorbed through any of the global reactions R2–R4 [41, 45]. CO_2 may be bound as carbonate, bicarbonate and carbamate depending on the operational conditions of the absorber. The reaction enthalpy (ΔH in kJ/mol CO_2) of the global reactions reflects the energy released when CO_2 is absorbed in the liquid. From an enthalpy of reaction perspective, it is preferable to absorb CO_2 through reactions R2 (bicarbonate) and R4 (carbamate) rather than through reaction R3 (carbonate). In the work performed by Qin et al. [45], the heat of absorption was measured at 40°C and 2.5 wt% NH_3. At CO_2 loadings in the range of 0.0–0.6, the heat of reaction was 60–80 kJ/mol CO_2. This indicates that the absorption is governed by R4, and to some degree R2 and R3. In Paper III, the global reactions (R2–R4) are used to motivate the preferred operating conditions in which the heat requirement is reduced.

$$NH_3(aq) + CO_2(g) + H_2O \rightleftharpoons NH_4^+ + HCO_3^- \qquad \Delta H = 64.26\ kJ/mol\ CO_2 \qquad \text{(R2)}$$

$$2NH_3(aq) + CO_2(g) + H_2O \rightleftharpoons 2NH_4^+ + CO_3^{2-} \qquad \Delta H = 101.22\ kJ/mol\ CO_2 \qquad \text{(R3)}$$

$$2NH_3(aq) + CO_2(g) \rightleftharpoons NH_4^+ + NH_2COO^- \qquad \Delta H = 72.32\ kJ/mol\ CO_2 \qquad \text{(R4)}$$

3.3. Experimental work on the NH_3-CO_2-H_2O system

Equilibrium

Experimental work on the ternary NH_3-CO_2-H_2O system dates back to the end of the 1920's. The focus of much of the early work was to determine the equilibrium composition of the system. In the work conducted by Jänecke et al. [46] from 1929, the possible solid-phase species of the system were identified. Most of the experimental data on the NH_3-CO_2-H_2O system are available for the gas-phase composition at the VLE. During the last 20 years, there have also been some developments with respect to determining the carbon distribution in the liquid phase. Figure 3.5 shows a graphical representation of the conditions for which experimental data on equilibrium species distributions have been reported in the literature for the vapor phase (a) [24, 47-56] and the liquid phase (b) [57-61]. For each experimental data-point, there are two symbols, one for the ammonia molality (crosses) and one for the CO_2 molality (triangles). The purpose of Figure 3.5 is to show where thermodynamic models

based on the data listed below can be expected to show predicitve capabilities. Comparing the temperature levels and ammonia and CO_2 concentrations in Figure 3.5 to conditions that can be expected in a ammonia-based, post-combustion capture process, it becomes evident that there are more experiemtal data for the stripper conditions (100°–150°C) than for the absorber condistions (0°–20°C) - there are few expermental data-points below 20°C. That there is a need for further experimental data is the premise of Paper I. The red symbols in Figure 3.5 denote the experimental conditions used in Paper I.

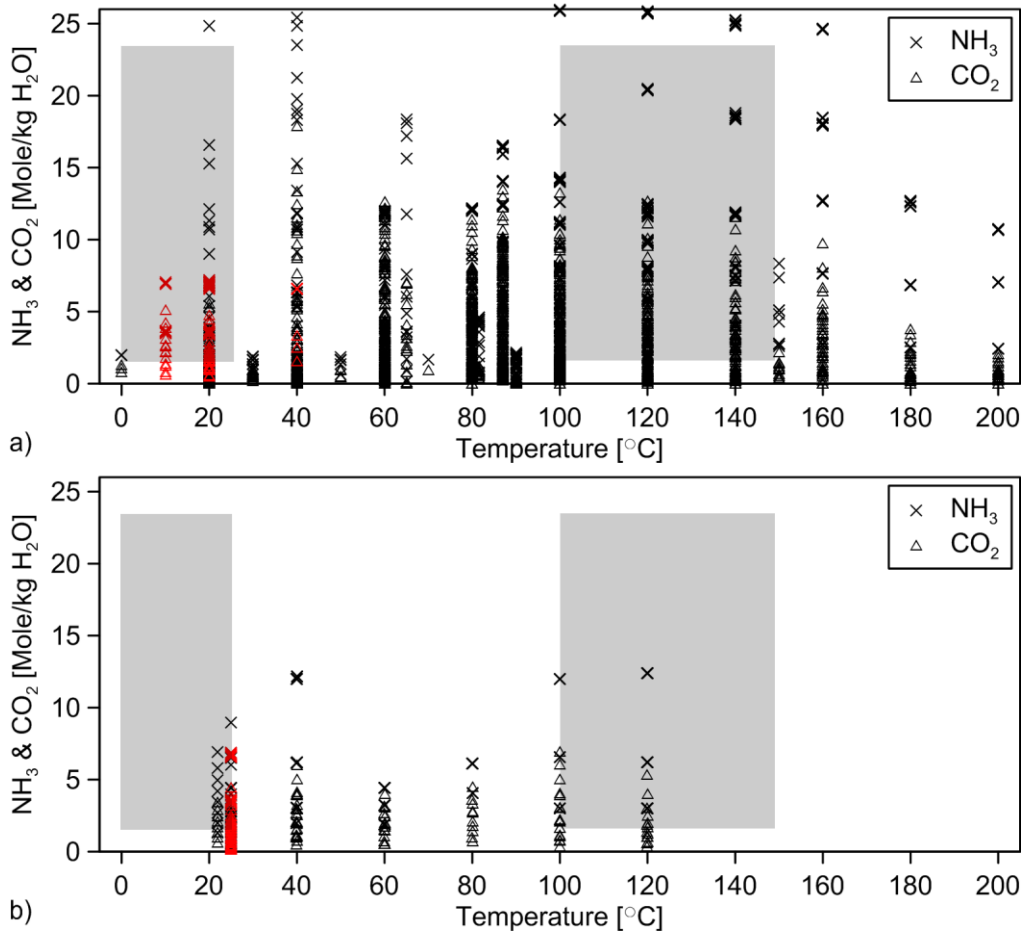

Figure 3.5 Graphical representation of the conditions for which experimental vapor-liquid equilibrium data exist for the liquid phase (a) and gas phase (b). The shaded areas, for the ranges of 0°–20°C and 100°–150°C, represent the operating conditions of the absorber and the stripper, respectively. Each ammonia concentration is represented by a cross and each CO_2 concentration is represented by a triangle. The red symbols denote the experimental conditions used in Paper I. Source: Paper I.

In Paper I, gas chromatography and Raman spectroscopy are used. However, other experimental methods can be used to evaluate the gas and liquid compositions at the VLE. The gas composition can be measured by gas absorption and back-titration [53] or by gas chromatography with a thermal conductivity detector [48, 49, 55]. Gas chromatography has been the method of choice since the 1980's. However, this methodology has not been applied for operational temperatures of <40°C. Different experimental measurement techniques can be used to determine the carbon distribution in the liquid phase, including nuclear magnetic resonance (^{13}C-NMR) and Raman spectroscopy. Both of these techniques have been used in previous studies. For example, Ahn et al. [59], Mani et al. [62], and Holmes et al. [60] have used ^{13}C-NMR, while Wen and Brooker [61], Zhao et al. [58], and Paper A have used Raman spectroscopy. All these experimental studies were performed at close to room temperature.

Reaction kinetics

For the absorption of CO_2 to aqueous ammonia, the carbamate and bicarbonate formation reactions (R5 and R6) are considered to be rate-determining [63]. According to the equilibrium speciation data presented in Paper I, CO_2 is predominantly bound as carbamate at low CO_2 loadings. The formation of bicarbonate is the main reaction that increases the CO_2 loading to >0.5. The bicarbonate formation reaction (R6) has been investigated in the work of Pinsent et al. [64]. Carbamate formation can be regarded as the main reaction route for CO_2 absorption at CO_2 loadings <0.5. The carbamate reaction may be represented by either a two-step zwitterion mechanism (R7–R8) [65-67] or an Arrhenius expression (R5) [68, 69]. In R7 and R8, the letter 'B' denotes any base that is present in the liquid solution. Figure 3.6 shows the measured apparent kinetic rate of the carbamate formation reaction in five investigations as a function of temperature. The apparent reaction rate for the corresponding carbamate formation reaction in an MEA-based absorption process, as given by Versteeg et al. [70], is also included in Figure 3.6. The operating conditions are a CO_2-free solution with an ammonia concentration of 1 kmol/m^3. It is apparent from Figure 3.6 that there is no consensus with respect to the apparent reaction rate or even the temperature dependence of the carbamate reaction. However, the absorption rate of ammonia is likely to be slower than that of MEA. Figure 3.6 also includes a "Log. mean" reaction rate, which is proposed in Paper II. Due to the large discrepancy between the experimentally determined reaction rates, a logarithmic mean, "Log. mean", between the most extreme reaction rates of Pinsent et al. [68] and Puxty et al. [69] is calculated. All three of these reaction rates are used in Paper II for the validation of a suitable absorber model. One reason for the large discrepancy between the sources could be the use of different experimental apparatuses to determine the carbamate reaction rates. The experimental apparatuses used were a wetted wall column [67, 69], a string of discs contactors [66], a stirred cell reactor [65] and a bubble reactor [68].

$$NH_3(aq) + CO_2(aq) + H_2O \rightarrow NH_2COO^- + H_3O^+ \quad \text{(R5)}$$

$$CO_2(aq) + OH^- \rightarrow HCO_3^- \quad \text{(R6)}$$

$$CO_2 + NH_3 \leftrightarrow NH_3^+COO^- \quad \text{(R7)}$$

$$NH_3^+COO^- + B \leftrightarrow NH_2COO^- + BH^+ \quad \text{(R8)}$$

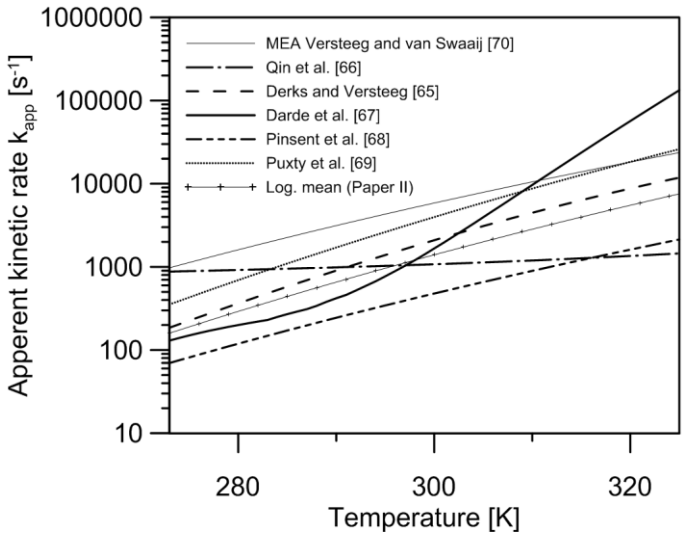

Figure 3.6 Apparent kinetic reaction rates for carbamate formation (R5 and R7-8) as a function of temperature (molarity basis). The conditions correspond to a CO_2-free solution with an ammonia concentration of 1 kmol/m^3. The reaction rates described by Puxty et al. [69] and Pinsent et al. [68] and the "Log. mean" use an Arrhenius expression, while the remaining rates [65-67] are expressed as two-step zwitterion mechanisms. The apparent kinetic reaction rate for the MEA carbamate reaction is taken from Versteeg and van Swaaij [70]. Source: Paper II.

3.4. Modeling of the NH_3-CO_2-H_2O system

Equilibrium-based

As the NH_3-CO_2-H_2O system is a mixture of molecular species and non-volatile ionic compounds, a detailed thermodynamic model framework is required to determine the phase behavior and composition. The liquid phase of an electrolyte solution requires an activity coefficient model to describe the interionic forces and the non-ideal behavior of the solution. An equation of state is also required to describe the vapor phase behavior, i.e., to calculate the fugacity coefficients. Thermodynamic models that describe the NH_3-CO_2-H_2O system have been established by Darde et al. [71] and Que and Chen [72]. Common to these two thermodynamic models is the treatment of the VLE of ammonia, CO_2, and water. In general, the liquid-phase chemistry is determined by following five ionic equilibrium-based reactions (R9–R13). The precipitation of ammonium bicarbonate $NH_4HCO_3(s)$ is included in all the models (R14). The equilibrium composition is determined by equilibrium constants for all the reactions (R9–R14), and the activity coefficient accounts for the non-ideality of the mixture.

Eq.	$H_2O \leftrightarrow H^+ + OH^-$	(R9)
Eq.	$NH_3 + H_2O \leftrightarrow NH_4^+ + OH^-$	(R10)
Eq.	$CO_2 + H_2O \leftrightarrow HCO_3^- + H^+$	(R11)
Eq.	$HCO_3^- \leftrightarrow CO_3^{2-} + H^+$	(R12)
Eq.	$NH_3 + HCO_3^- \leftrightarrow NH_2COO^- + H_2O$	(R13)
Eq.	$NH_4^+ + HCO_3^- \rightleftharpoons NH_4HCO_3(s)$	(R14)

However, the model developed by Darde et al. [71] also includes the solid states of ammonium carbonate $(NH_4)_2CO_3(s)$, ammonium carbamate $NH_2COONH_4\,(s)$, and ammonium sesqicarbonate $(NH_4)_2CO_3 \cdot NH_4HCO_3(s)$. The thermodynamic model presented by Darde et al. [71] is based on the extended UNIQUAC electrolyte model developed by Thomsen and Rasmussen [73]. The model of Darde et al. [71] has been used extensively in process simulations of both the CAP and AAP [32, 44, 74, 75]. This model is also used in Paper I, to evaluate its predictive capabilities against the experimental data. The thermodynamic model of Que and Chen [72], used in Papers I–V, employs the electrolyte NRTL model developed by Chen et al. [76]. The electrolyte NRTL is the default electrolyte model used by the Aspen Plus v8.0 process simulation software.

Rate-based

Simulations of reactive processes that are limited by the reaction kinetics require a rate-based approach. Equilibrium simulations of such processes, e.g., the absorption, may lead to misleading conclusions. However, the absorption in post-combustion capture is fast enough to be characterized as liquid-film-controlled if a two-film assumption is used [66]. Thus, the bulk liquid is characterized by a low reactivity. Reactions R15–R22 show the rate-based reaction mechanism used in the NH_3-CO_2-H_2O system in the Aspen Plus process simulation software. In comparison to the equilibrium-based reaction mechanism (R9–R14), the forward and backward reaction rates for carbamate (R18–R19) and bicarbonate (R20–R21) replace R13 and R11, respectively [63]. The default rates in Aspen Plus for all the reactions are taken from the studies of Pinsent et al. [64, 68]. However, in Paper II, the reaction rates of Puxty et al. [69], the "Log. mean", are evaluated as being representative of the forward and backward carbamate reactions (R18–R19).

Eq.	$H_2O \leftrightarrow H^+ + OH^-$	(R15)
Eq.	$NH_3 + H_2O \leftrightarrow NH_4^+ + OH^-$	(R16)
Eq.	$HCO_3^- \leftrightarrow CO_3^{2-} + H^+$	(R17)
Rate	$NH_3 + CO_2 + H_2O \rightarrow NH_2COO^- + H_3O^+$	(R18)
Rate	$NH_2COO^- + H_3O^+ \rightarrow NH_3 + CO_2 + H_2O$	(R19)
Rate	$CO_2 + OH^- \rightarrow HCO_3^-$	(R20)
Rate	$HCO_3^- \rightarrow CO_2 + OH^-$	(R21)
Eq.	$NH_4^+ + HCO_3^- \rightleftharpoons NH_4HCO_3(s)$	(R22)

3.5. Present status of the field

Even though CO_2 absorption into aqueous ammonia has been a subject of research for many decades, there are still areas in which advances are required. With respect to the experimental data on the NH_3-CO_2-H_2O system, there are abundant data on the equilibrium gas-phase composition, and far less data on the liquid-phase composition. With respect to the solid phase since 1929, very little, if any, dedicated work has been conducted on the precipitation behavior of the NH_3-CO_2-H_2O system. There is a lack of VLE data at low temperatures (<20°C), and this is a crucial temperature range for both the CAP and the AAP. Thus, there is a need to produce more VLE data over a wider range of temperatures. Two primary thermodynamic models are currently used for process simulations of the CAP and the AAP: the models of Darde et al. [71] and Que and Chen [72]. It is unclear which of the models that has the most accurate predictive capability. In addition, many studies have been performed on evaluating the absorption reaction rate of CO_2 in aqueous ammonia. However, the discrepancies between the sources are significant and it is unclear as to how these discrepancies affect the design of the absorber. There have been many simulation studies of the CAP and AAP in which absorption has been considered with an equilibrium assumption. These studies show good consensus, with a heat

requirement of around 2,500 kJ/kg CO_2. However, there are still few published studies in which the absorption has been treated with rate-based simulations, and it remains unclear as to how the discrepant absorption reaction rates affect the results. In this context, pilot plant operation data can offer some insights. Among the nine reported pilot plants, only the work conducted by CSIRO [30] provides pilot plant data that is sufficiently detailed to facilitate any type of process simulation validation. This is also one of few studies in which the pilot plant design of an AAP is presented. However, there is a need to gather state-of-art experience and evaluate the cost of capture of a full-scale AAP when it is attached to an existing process.

4. Methodology

This thesis evaluates various aspects related to the use of ammonia as an absorbent of CO_2. Figure 4.1 shows a schematic overview of the relationships between the methods applied in this work. The methodologies range from measuring the properties of the NH_3-CO_2-H_2O system to estimating the capture cost for the AAP process. Modeling the capture process relies on thermodynamic models with strong predictive capabilities. Thermodynamic models of mixtures that include electrolytes are inherently difficult to describe theoretically, and require a thorough experimental basis. Highly important are the data on the gas- and liquid-phase compositions. In Paper I, the gas-phase CO_2 concentration and the liquid-phase carbon distribution are measured under the conditions for the absorption, which is not covered in any previous work. The measured data are compared with existing thermodynamic models to validate their capabilities to describe the system. The chosen thermodynamic model is applied to describe the individual units of the capture process. Paper II evaluates the design of the absorber with respect to capture efficiency, ammonia slip, and absorber height. Paper III evaluates the heat requirement for the ammonia regeneration process (CO_2 desorption) and proposes operational conditions that entail a low heat requirement. The issue of how to control ammonia slip is dealt with in Paper IV. This paper evaluates different ammonia control options and the conditions under which ammonia slip can be controlled most efficiently. Paper IV is closely related to the overall aim of the thesis, as it is the ammonia slip that dictates or sets the limits for when ammonia-based, post-combustion capture is favorable. In Paper V, a favorable CO_2 source is integrated with the AAP. A coal-fired power plant is chosen as a suitable reference plant. In this paper, all the experience gained from previous studies is utilized to construct a detailed, full-size process that includes unit dimensions and thermal integration with the power plant. The detailed process description is then used to estimate the CAPEX and OPEX of the capture process. The final stage of the overall methodology of this thesis is to estimate the cost for CO_2 capture. The column to the right in Figure 4.1 divides the methodologies into six categories. A detailed discussion of these categories is provided below.

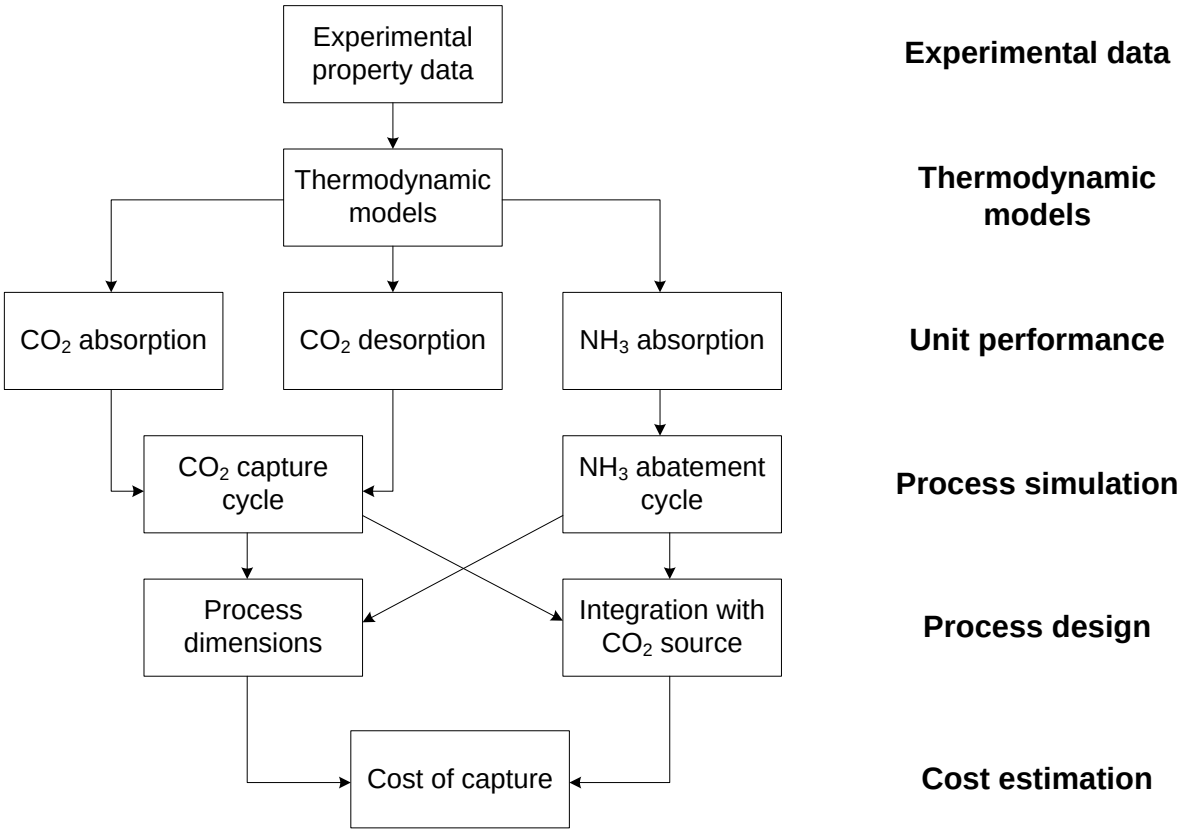

Figure 4.1 Schematic overview of the methodologies applied in this thesis.

4.1. Validation of thermodynamic models

Paper I presents new experimental data series in the range of 10°–40°C, 5 wt% and 10 wt% ammonia, and CO_2-loadings in the range of 0.00–0.75. The experimental procedure determines the carbon distribution in both the gas and liquid phases. The equilibrium partial pressure of CO_2 is determined by gas chromatography (Figure 4.2a). The operating conditions of the gas chromatograph are presented in Paper I. The carbon distributions in the liquid phase are categorized into carbonate (Figure 4.2b), bicarbonate (Figure 4.2c), and carbamate (Figure 4.2d). The liquid-phase distributions are determined by Raman spectroscopy. The liquid speciation methodology employed in Paper I is presented in the *Appendix* (Paper A). The method is based on partial-least-squares regression of the Raman spectra. Figure 4.2 shows some of the experimental data that are presented in Paper I. The operating conditions are 10 wt% ammonia (CO_2-free) and CO_2-loadings in the range of 0.00–0.75. The gas-phase samples are extracted at 20°C, and the liquid-phase samples are scanned at 25°C. The experimental data are validated with the existing thermodynamic models of Darde et al. [71] and Que and Chen [72]. In this work, no regression of new interaction constants in the thermodynamic modeling framework is performed. Thus, this work merely evaluates the extrapolation capabilities of the existing models. Much of the data presented in Figure 3.5 have been used in the regression of both models. The predictions made by the model of Que and Chen prove overall to be the most accurate for the gas-phase CO_2 predictions. With respect to the liquid-phase predictions, there is a much larger discrepancy between the experimental sources. However, the general trends of the model prediction are correct for all species. With respect to the liquid phase, more work needs to be done to produce more accurate predictions. There is a large discrepancy between the different sources used to determine the liquid carbon distributions, and this complicates any new attempts at regression. In the process modeling shown in Papers II–V, the model of Que and Chen [72] is used.

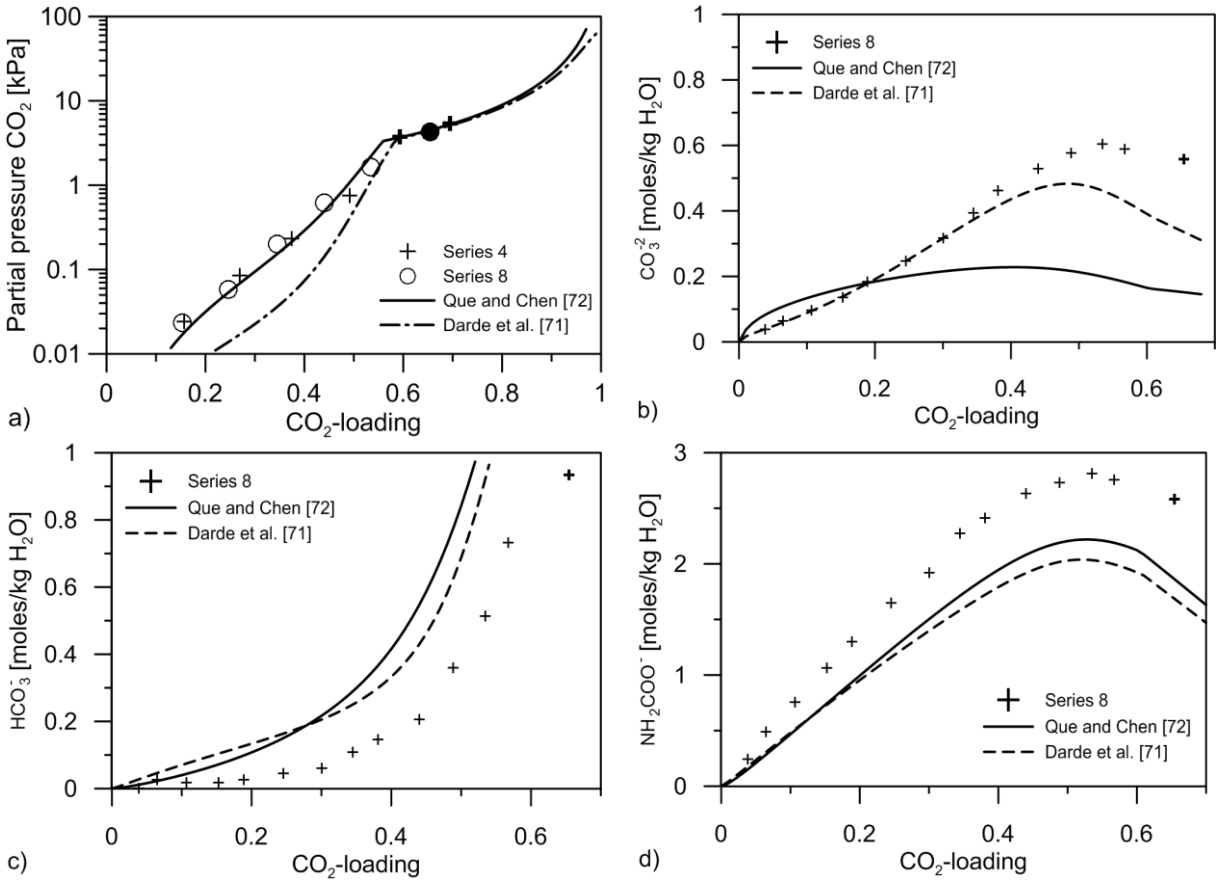

Figure 4.2 Experimental data obtained at 10 wt% NH_3 and CO_2-loadings in the range off 0.00–0.75 (measurement series 4 and 8 in Paper I). a) Partial pressure of CO_2; b) molality of carbonate; c) molality of bicarbonate; d) molality of carbamate. The gas-phase data are produced at 20°C (a), and the liquid-phase data are produced at 25°C (b–d). The experimental data are compared with predictions derived from the models of Darde et al. [71] and Que and Chen [72]. The bolded symbols indicate sample in which precipitation was noted. Source: Paper I.

4.2. Process simulations

Process simulations conducted in this work include both the evaluation and design of individual units in the AAP process, the AAP processes, and the integration of the AAP process with a power plant. The simulations of individual unit operations include the performances of the absorber, stripper, and wash unit. Assumptions regarding auxiliary units, such as heat exchangers, pumps, compressors, and buffer tanks, are presented in Paper V. However, the column simulation considerations are presented below, as this is an important aspect for the capture process and it is treated differently in the appended papers.

Column simulations

Various modeling procedures can be applied to simulate absorber operation. Simulation studies of the CAP and AAP have included the following models to represent the absorber: equilibrium flash-tank model [38, 41], equilibrium-based multistage model [32, 37, 44], and rate-based multistage model [34, 77]. The flash-tank model assumes isothermal equilibrium in one stage, which means that both the bulk liquid and vapor phases are assumed to be perfectly mixed and in equilibrium, and it is assumed that the interface between the two phases is in equilibrium. The thermodynamic models (described in Chapter 3.4) are used to determine the equilibrium composition of the bulk phases. In this thesis and in Papers II–V, the thermodynamic model of Que and Chen is used [72]. In the equilibrium-based multistage model, the absorber is divided into several equilibrium stages, just as in the flash-tank model, with the difference being that the stages are non-isothermal. During rate-based simulations, the reaction rates in the liquid film interface are considered. The thickness of the liquid film is determined by a mass transfer correlation based on dimensionless numbers. A commonly used mass transfer correlation for packed columns is the one described by Onda et al. [78]. At each stage, the two-film theory is employed for the bulk gas phase and the bulk liquid phase. Figure 4.3 illustrates how the absorber is divided into stages along the height of the absorber. As stated earlier, the CO_2 is chemically bound through reaction with the ammonia in the liquid film. In the Aspen Plus software, the liquid film is discretized over the thickness of the film, as shown in Figure 4.3. To ensure coverage of the gradient close to the gas-liquid interface, the segments are narrower than they are in the remainder of the liquid film.

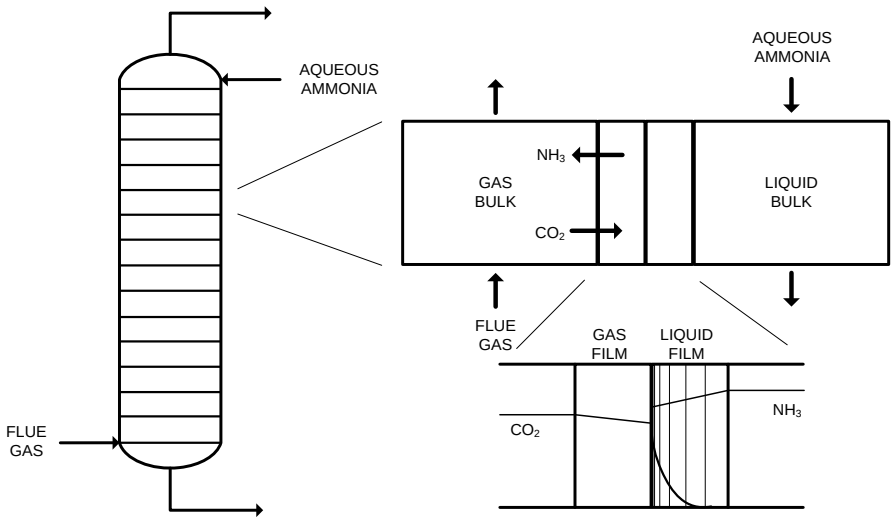

Figure 4.3 Schematic of the modeling strategy used for multistage rate-based column simulations. The column is divided into stages along the height of the absorber. At each stage, the two-film theory is applied to describe the interactions of the gas and liquid phases. The liquid film between the bulk phases is discretized to account for the reactions occurring in the film.

The absorber in Papers II, IV and V are represented by rate-based simulations. The "Log. mean" reaction rate presented in Paper II is used to represent the carbamate reaction (R18-19) in the film. The reaction rate of the bicarbonate formation (R20-21) has been designated as the default by Pinsent et al. [64]. This absorber modeling setup is in Paper II validated against the experimental pilot plant data reported by Yu et al. [30]. In Paper III, the absorber is represented by a flash-tank model. However, in Paper III, the aim is to evaluate the heat requirement for regeneration rather than the absorption process. The water wash is simulated with the same rate-based approach as the absorber, as they involve the same cold conditions. The stripper in Papers III and IV and the ammonia stripper in Papers IV and V are all represented by equilibrium-based columns. The effect of using an equilibrium-based

rather than a rate-based column to simulate the absorption is discussed in Chapter 6.2. It is assumed that owing to the hot conditions, the state of the process will be close to equilibrium. Also, there are no reported reaction rate data for temperatures >40°C and both strippers operate at temperatures >100°C. Thus, there is no support for rate-based simulations under these conditions.

Process flow sheets

The process simulations of the entire capture process are divided into four different simulation flow-sheets (Processes A–D in Figure 3.1). All simulations are performed in the process simulation software Aspen Plus v8.0 (v7.3.2 in Paper III). The flue gas pretreatment (Process A) and the CO_2 compression (Process D) are modeled as once-through flow-sheets. However, the CO_2 capture cycle (Process B) and the ammonia abatement cycle (Process C) are modeled as closed loops. Both of the latter processes consist of an inner loop formed by the rich/lean heat exchanger and the stripper plus an outer loop that encompasses all the units. The default sequential Broyden process solver is used to converge the simulations. The convergence tolerance is set at 10^{-6} for the inner loop and 10^{-5} for the outer loop. The lean CO_2 stream is set as the tear stream. A make-up stream is added to the CO_2 lean stream to account for the losses of ammonia and water.

Process design

To estimate the investment cost of a full-scale, ammonia-based capture process, a detailed equipment list is required. In Paper V, a detailed description of the process schematic and assumption is presented. Most of the process data can be garnered from the process simulations, while the remainder requires the making of assumptions based on experience data from the literature. Most of the process dimensions can be related to those of the MEA-based process. Paper V only provides a full-scale process description, but also suggests possible cost reduction designs for the capture process. It suggests that cost reductions can be made by considering different design options for the absorber packing material and the rich/lean heat exchanger design. As the rich/lean heat exchanger is a capital-intensive unit in any post-combustion capture process, there is a need to reduce the cost. The most intuitive design of the rich/lean heat exchanger would be to use a shell-and-tube heat exchanger, owing to the high pressure and the risk of precipitation. In Paper V, an alternative design for the rich/lean heat exchanger, using a plate-and-frame heat exchanger, is evaluated. A plate-and-frame heat exchanger not only reduces the cost by 75%, but also the heat transfer coefficient is increased two-fold. Another potential cost reduction measure is to change the packing material of the absorbers. The benchmarking packing material in the MEA process is a metallic structured packing. It is proposed in Paper V to change the column packing material to a plastic packing. Plastic packing cannot be used in the MEA process because temperature peaks of up to 80°C would cause permanent deformation of the plastic. The peak temperature in the ammonia process is only 40°C, assuming the availability of cold cooling water. Plastic packing is 90% cheaper than metallic packing material.

In of ammonia-based, post-combustion capture, it is important to design the process so as to reduce the ammonia slip using both primary and secondary measures. The 10 ppm limit for discharge of ammonia to the atmosphere is the strictest design limitation for the process. Primary ammonia recovery methods reduce the ammonia slip already from the absorber, whereas secondary measures reduce the gas-phase concentration of ammonia downstream of the absorber. Absorber operating conditions that reduce ammonia slip are presented in Chapter 5.1. As no primary measure has the capability to reduce the ammonia slip to allowable levels, a secondary measure is always required. Paper IV evaluates three different combinations (Designs) of ammonia control methods:

- Case 1: Staged absorption + Ammonia abatement cycle
- Case 2: Staged absorption + Chilled absorption + Ammonia abatement cycle
- Case 3: Staged absorption + Chilled absorption + Acid wash

All three designs have the ability to reduce the ammonia slip to 10 ppm. The present methodology will be used to determine the consumption of utilities (electricity, steam, cooling water, and make-up chemicals) for each reduction method.

Process integration with a power plant

The premise of Paper V is the integration of ammonia-based, post-combustion capture with a full-scale CO_2-emitting point source. The reference process in this case is the Danish coal-fired power plant Nordjyllandsvearket (NJV), which has an electric generation capacity of 408 MW_{el}. In its present state (without capture), this power plant is characterized by a high electric efficiency (47%) due to its access to low-temperature cooling water, double reheat cycles, and advanced feed water preheating system. The capture process is attached to the power plant at the end of the current flue gas cleaning system. The steam from the intermediate pressure part (IP0, 7.2 bar; and IP1, 1.5 bar) is extracted to feed the carbon capture cycle and the ammonia abatement cycle. The penalty for the power plant is the loss of electricity production, which arises from the loss of steam and the internal use of electricity for compression and pumping operations. The power plant penalty will eventually result in a decrease in the electric efficiency of the power plant

4.3. Cost estimations

Cost estimations have been applied in Papers IV and V. The economic analysis is based on the use of the net present value method (NPV) to determine the capital expenditure (CAPEX) and the operating expenditure (OPEX). In Paper V, a detailed equipment list is established for the AAP at a coal-fired power plant. The investment cost of each unit is estimated using the Aspen In-Plant Cost Estimator. An individually determined installation factor is then applied to estimate the CAPEX for each unit. The OPEX is divided into the following categories: annualized capital cost; maintenance; labor; and utility costs. The utility cost consists of the costs for steam, electricity, chemical make-up, and cooling water. In Paper V, both the CAPEX and OPEX are calculated, whereas in Paper IV, a simplified economic evaluation method is used in which only the utility cost of reducing the ammonia slip is evaluated. Table 4.1 lists the assumptions made in the economic analysis. In Paper V, the loss of primary steam is regarded as loss of electricity revenue (spot price). As Paper IV represent a more general case, all utilities (including steam and electricity) need to be purchased from the marketplace. The spot and market prices for electricity are taken as an average of the electricity prices in Europe in the period 2010–2013 [79].

Table 4.1 Cost assumptions ($€_{2013}$) used in the economic estimations.

Interest rate	7.5%
Economic life-time	25 years
Power plant operating hours	8000 h/year
Contingency investment cost	25%
Maintenance	4% of capital cost/unit/year
Labor	Six Operators at 56 €/h and one Engineer at 69 €/h during hours of operation
Electricity (spot price)	50 €/MWh
Electricity (market price)	100 €/MWh
Steam	12.5 €/ton
Cooling water	0.025 €/m^3
Ammonia	400 €/ton
Sulfuric acid	45 €/ton

5. Evaluation of Unit Operations of the AAP

The focus of this chapter is to present the results of an evaluation of the essential units of the AAP. Using process simulations, suitable operating conditions are suggested and discussed. The evaluated units are: the absorption process; the desorption process; and the ammonia control method. The evaluation is not only based on the technical aspects, but also the economic aspects. The present chapter includes results from Papers II–IV.

5.1. Absorption column

In the absorber, aqueous ammonia is distributed over a packing material from the top of the column. The flue gases are introduced at the bottom of the column. The primary role of the absorber is to absorb as much CO_2 as possible using as little solvent as possible, while simultaneously minimizing the slip of ammonia. Figure 5.1 shows the CO_2 capture efficiencies along the height of the absorber for various absorber loadings (mole-ratio of CO_2 in the flue gases and the ammonia in the CO_2-lean stream). The figure highlights the difference in the reaction rates for carbamate (R18) and bicarbonate (R20) formation. For absorber loadings of 0.25 and 0.33, there is a sharp trend change at around the 10 mark. At a height of <10 m in the absorber, the absorption is governed by the fast carbamate reaction, whereas at heights >10 m, the absorption is governed by the slow bicarbonate reaction. The change in trend can be attributed to the liquid-phase CO_2-loading reaching 0.5, as denoted by crosses in Figure 5.1. For an absorber loading of 0.2, the CO_2-loading only reaches 0.49 but the capture efficiency is 99.7% at an absorber height of 40 m. Thus, for efficient operation, the absorber loading should be adjusted so that the CO_2-loading reaches 0.5 at the desired capture efficiency. The rate of absorption at CO_2-loadings >0.5 is too slow. Figure 5.1 also shows the corresponding equilibrium capture efficiencies at absorber loadings of 0.20, 0.25, and 0.33. The equilibrium capture efficiencies at 0.20 and 0.25 are very close to 100%, although at an absorber loading of 0.33 the capture efficiency is around 94%. Thus, almost 30% more CO_2 could be captured in the absorber at infinite residence time. As a reference, the absorber loading in Paper III is set to a constant value of 0.5.

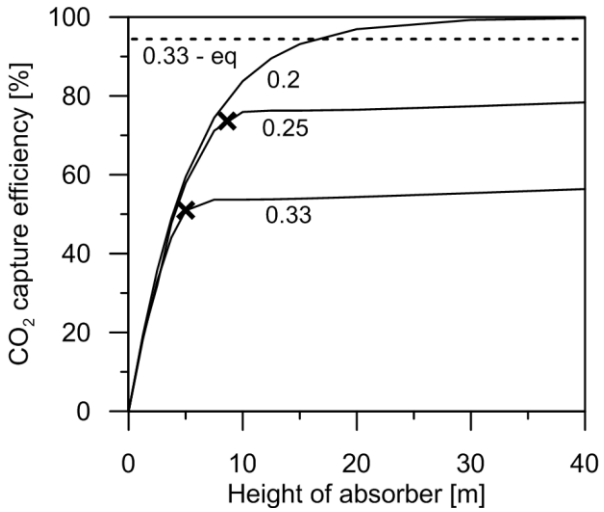

Figure 5.1 CO_2 capture efficiency of the absorber as a function of absorber column height. The capture efficiencies are shown for absorber loadings of 0.33, 0.25, and 0.20. The carbamate reaction (R18) is represented by the "Log. mean" reaction rate (solid lines). The dashed line represents the capture efficiency at equilibrium with an absorber loading of 0.33. The capture efficiencies at equilibrium for absorber loadings of 0.25 and 0.20 are close to 100%. The crosses indicate CO_2-loadings of 0.5. The ammonia concentration and CO_2-loading are constant at 10% and 0.25, respectively. Source: Paper II.

One of the major uncertainties in this thesis is the rate of the carbamate reaction. This is related to Figure 3.6, which shows the apparent reaction rate of the carbamate reaction, as suggested by different sources. In Paper II, the reaction rates reported by Puxty et al. [69] and Pinsent et al. [68], and the logarithmic mean (Log. mean) of these two values are compared with the pilot plant data reported by Yu et al. [30]. The reaction rates determined by Puxty et al. [69] and Pinsent et al. [68] overestimate and underestimate, respectively, the capture efficiency. The Log. mean provides the most accurate prediction. In Figure 3.6, the reaction rates of Puxty et al. [69] and Pinsent et al. [68] represent both the fastest and the slowest of the reported reaction rates. Figure 5.2 illustrates the effect of uncertainty regarding the carbamate reaction on the absorber design, i.e., the height of the absorber column. This figure shows rate-based simulations of an absorber for which the capture efficiency is set at 90% and the rich CO_2-loading is set at 0.5. The required absorber heights for the different reaction rates are 10 m [69], 15 m (Log. mean), and 22 m [69]. This shows that the uncertainty with respect to absorber height is roughly12 m. In Papers II, IV, and V, the absorber height is set at 15 m.

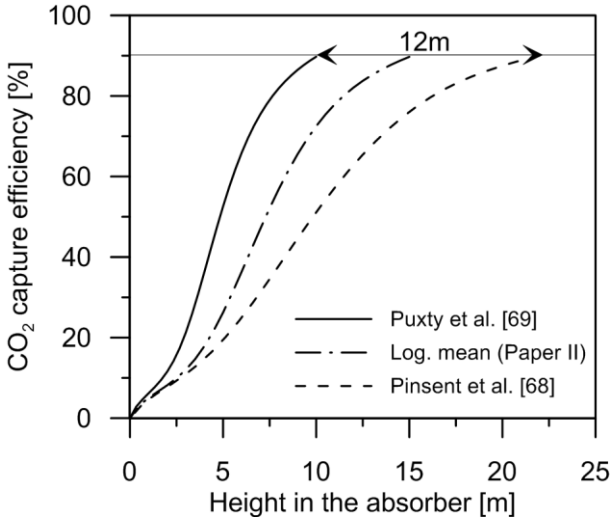

Figure 5.2 Capture efficiencies along the height of the absorber for three different reaction rates for carbamate formation (R18). The capture efficiency is set at 90% and the rich CO_2-loading is set at 0.5. The ammonia concentration and lean CO_2-loading are constant at 10% and 0.25, respectively.

A secondary goal is to minimize the loss of absorbent. This is especially important in ammonia-based, post-combustion capture as ammonia is volatile. The conditions at the top of the absorber dictate the slip of ammonia. The conditions at the top stage of the absorber are going to be close to that of the CO_2-lean stream. Figure 5.3 show the equilibrium ammonia partial pressure as a function of CO_2/NH_3 ratio (CO_2-loading), ammonia concentration (a), and temperature (b). The operating pressure of the absorber is set to that of the atmospheric condition (100 kPa). A common design target is to use a CO_2-loading of 0.25 in the lean stream and to use as low an operating temperature as can be achieved using the available cooling water. The ammonia concentration should be sufficiently low to avoid precipitation and excessive ammonia slip, and high enough to avoid a liquid flow rate that is too high. In Papers II, IV, and V, an ammonia concentration of 15% (14.3wt%) is used. As shown in Figure 5.3b, the ammonia partial pressure is significantly reduced by ensuring a low operating temperature at the top of the absorber.

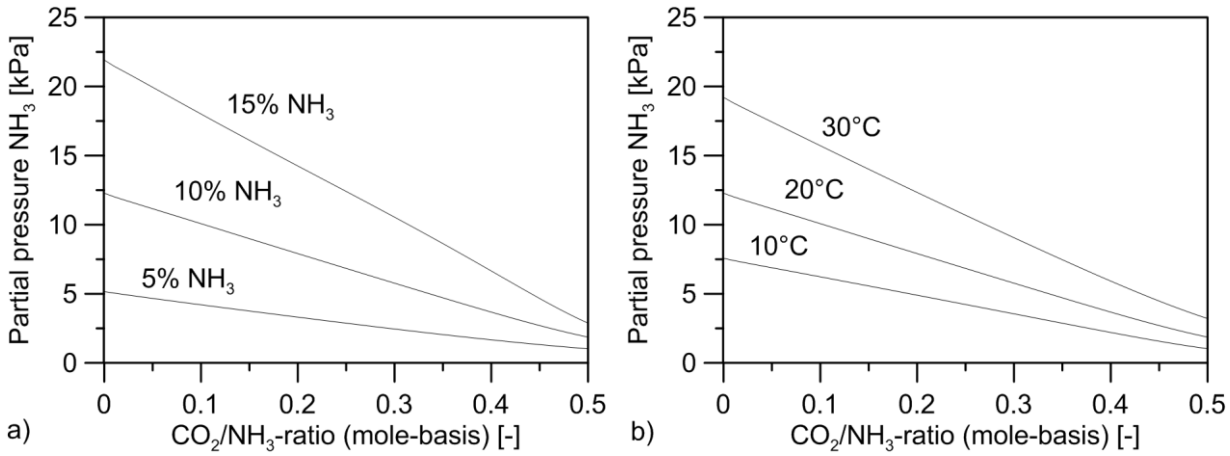

Figure 5.3 Equilibrium partial pressures of ammonia as a function of the CO_2-loading and the concentration of ammonia (CO_2-free) at a temperature of 20°C (a) and at 10% NH_3 (b). Based on the model proposed by Que and Chen [72]. Source: Paper IV.

Staged absorption

The major challenge in the design of an ammonia-based, post-combustion capture process is to reduce the ammonia slip. One option, which is presented in Paper II, significantly reduces the ammonia slip by employing staged absorption. Staged absorption relies on the fact that it is the top of the absorber that determines the ammonia slip. As mentioned earlier, the CO_2-loading of the lean stream is usually 0.25 and the rich CO_2-loading is limited to 0.5. By introducing a second absorber (A2) after the first absorber (A1) with intermediate intercooling, the conditions at the top of absorber A2 can be made significantly more favorable with respect to ammonia slip. Thus, the purpose of A1 is to absorb the majority of the CO_2. The CO_2-loading of the liquid stream is increased from 0.25 to around 0.5 in A1. By intercooling the rich stream, the conditions at the top of A2 are represented by a low temperature and a high CO_2-loading. As shown in Figure 5.3b, the ammonia partial pressure can be reduced by as much as three-fold by increasing the CO_2-loading from 0.25 to 0.5. Figure 5.4 shows two practical alternatives for the construction of a staged absorption system. Rate-based modeling of staged absorption is utilized in Papers IV and V. Using staged absorption will mimic the conditions of the equilibrium-based flash-tank, which is used to represent the absorber in Paper III. The conditions in the whole flash-tank will also be that of the rich stream, with the exception that the flash-tank will allow the CO_2-loading to exceed 0.5.

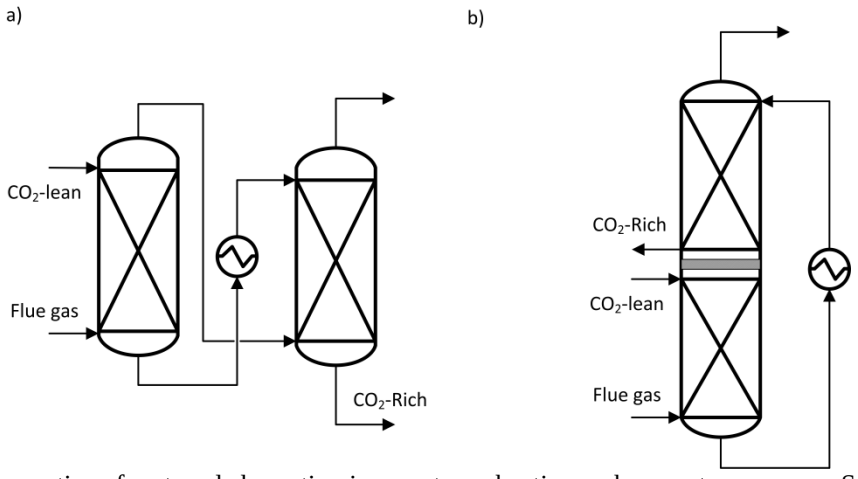

Figure 5.4 Design options for staged absorption in a post-combustion carbon capture process. Staged absorption can be achieved through either a two-absorber setup (a) or a pump-around system (b). Source: Paper II.

Figure 5.5 shows the CO_2 capture efficiency (a) and the ammonia slip (b) as a function of the absorber height. The data in the figure relate to a two-stage absorber and a common one-stage absorber. The total height of both setups is set at 20 m, although the two-absorber setup is divided into the A1 (15 m) and A2 (5 m) units. The liquid flow rate (L) is adjusted to achieve a capture efficiency of 90%. Absorber A2 can be shorter than A1, since ammonia absorption is faster than CO_2 absorption in A1. The total height of the absorber can be lower for a one-absorber setup, although the ammonia slip is around 5%. Staged absorption reduces the ammonia slip to around 3,000 ppm. The departure from equilibrium could even allow an ammonia slip below the equilibrium concentration. This can be the case if most of the ammonia is initially absorbed by carbamate. If the solution is able to reach equilibrium there will be a shift in the carbon distribution from being predominately carbamate to a larger proportion of bicarbonate. In this reaction, one mole of free ammonia is liberated.

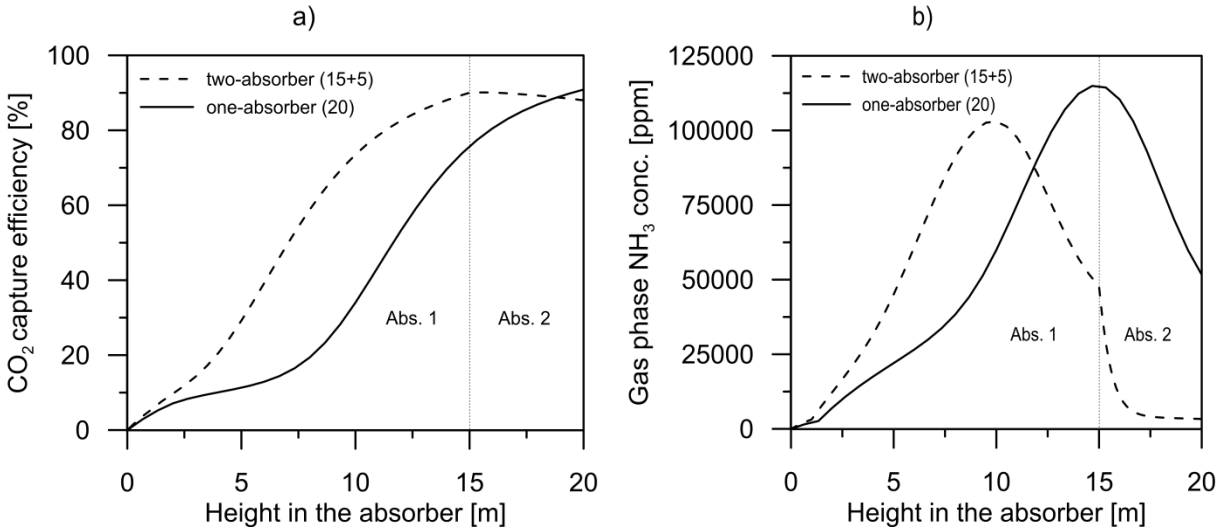

Figure 5.5 Gas-phase concentrations of CO_2 (a) and ammonia (b) along the height of the absorber, for the two different absorber configurations investigated (one-absorber and two-absorber). Both absorber set-ups have a total packed height of 20 m. In the two-absorber setup, the absorbers comprise a 15-m absorber and a 5-m absorber. Source: Paper II.

5.2. Stripper column

Some of the most important operating conditions of the stripper are the rich CO_2-loading, the temperature, and the pressure. The rich CO_2-loading is determined by the CO_2 capture capacity of the solvent and the conditions in the absorber. Ammonia has the capacity to reach a CO_2-loading of close to unity. At unity, almost all the CO_2 will be bound as bicarbonate (reaction R2), which has a low heat of absorption/desorption. Thus, a high rich CO_2-loading will result in a low heat requirement for regeneration. However, as previously mentioned, the rich CO_2-loading is limited to 0.5 in the absorber. The relationship between temperature and pressure in the stripper is illustrated in Figure 5.6. The figure is produced by calculating the equilibrium partial pressure for the NH_3-CO_2-H_2O system, for an ammonia concentration of 15%, CO_2-loading of 0.5, and vapor fraction of 0.05. These conditions are plausible operating conditions for the stripper. The temperature is varied between 70°C and 200°C and, as the vapor fraction is given, the total pressure is also calculated (top *x*-axis). The results can be related to the top of the stripper, while the temperature at the bottom of the stripper is usually 10°–15°C higher. The *y*-axis shows the relative flow of CO_2, i.e., how large are the flows of water and ammonia in relation to the flow of CO_2 under the specific conditions. Thus, the flow of CO_2 is assumed to be the same for all temperatures. As the temperature is decreasing, the shares of ammonia and water in the stripper off-gas are steadily increasing. At around 80°C, there are about equal amounts of all the gases in the CO_2 stream. The evaporation of water and ammonia requires heat, which increases the total heat requirement for regeneration, as the temperature decreases. For comparison, the slip of absorbent in the MEA process is almost negligible. However, the partial pressure of CO_2 in the MEA-CO_2-H_2O system is lower, entailing a higher level of water evaporation. The stripper pressure is also limited to 130°C due to the thermal degradation of absorbent. In Paper III, it is shown that the most significant difference between the ammonia and MEA processes with respect to the heat requirement is the extent of evaporation of water. Another positive effect of a high operating pressure is that less electricity is required for energy-intensive CO_2 gas compression. In both Paper III and Paper V, the stripper pressure is 20 bar. As presented in Figure 5.6, little is gained in terms of ammonia partial pressure reduction if the temperature and pressure settings are increased from 150°C and 20 bar to 180°C and 46 bar. The upper limit of the stripper pressure is determined by the structural difficulties and costs associated with the construction of a pressurized vessel of this size.

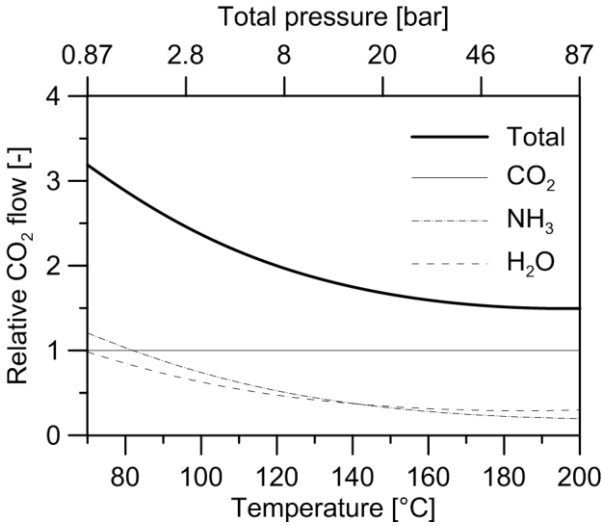

Figure 5.6 Equilibrium gas composition at an ammonia concentration of 15%, CO_2-loading of 0.5 and a vapor fraction of 0.05. The *y*-axis is presented as an index flow, whereby the flow of ammonia and water is related to the flow of CO_2. The total pressure is indicated by the top *x*-axis.

5.3. Ammonia control method

This chapter starts with a summary of the results from Paper IV, which evaluates different ammonia control methods. The evaluation method is based on which of the ammonia control methods has the lowest cost associated with utility consumption. The ammonia control design with the lowest cost will be used in the subsequent design of the AAP. The performances of the water wash and the ammonia abatement cycle are also evaluated in greater detail.

Choice of ammonia control method

Eventually, it is the cost of capture that will determine the success of any capture process. The largest uncertainly with respect to cost, when it comes to the operation of the AAP, is the cost of reducing the ammonia slip to the discharge limit of 10 ppm. In Paper IV, the three different ammonia control designs are evaluated. Each reduction case is evaluated for the range of conditions expected to be encountered at CO_2 emission sources. A high and a low case are represented for the flue gas CO_2 concentration (15% and 5%) and the cooling water temperature (5°C and 25°C). In Paper IV, a simplified economic analysis is used, in which only the utility cost of the ammonia control is estimated. The primary aim of the methodology is to quantify the share of the cost that needs to be allocated to the control of ammonia slip. This will eventually indicate the conditions under which the AAP is favorable. A secondary objective is to identify the most cost-efficient ammonia control design under the favorable conditions. The results presented in Figure 5.7 are the cost in Euro (Year 2013 level; $€_{2013}$) per tCO_2 that is captured. The utility cost of ammonia control is given per tCO_2, so as to be relatable to the total capture cost. As shown in Figure 5.7, the utility cost of ammonia control is penalized by high temperatures and low CO_2 concentrations. However, under the best-case conditions, the cost can be seen as reasonable. At flue gas CO_2 concentrations of around 15% and at cooling water temperatures of around 5°C, the utility cost can be as low as 1.5 €/tCO_2. These are the same conditions as are assumed for the reference power plant in Paper V. The total cost of capture is estimated to be 35.0 €/tCO_2. In the worst-case scenario, the utility cost of ammonia control is almost as high as the total capture cost in the best-case scenario. With respect to the different ammonia control designs, there is only a minor difference between Design 1 and Design 2. Thus, the ammonia abatement cycle with steam stripping reduction is the most cost-efficient ammonia control method. If chilled absorption is employed, the main concern will be the current electricity price in relation to the cost of steam production. The option to use a destructive method is the most expensive due to the high cost of ammonia replacement. The only case in which a destructive method may be used is if the residual ammonia can be used in the upstream flue gas cleaning system (SO_x or NO_x abatement). Thus, in the design described in Chapter 6, an ammonia abatement cycle with steam stripping will be used.

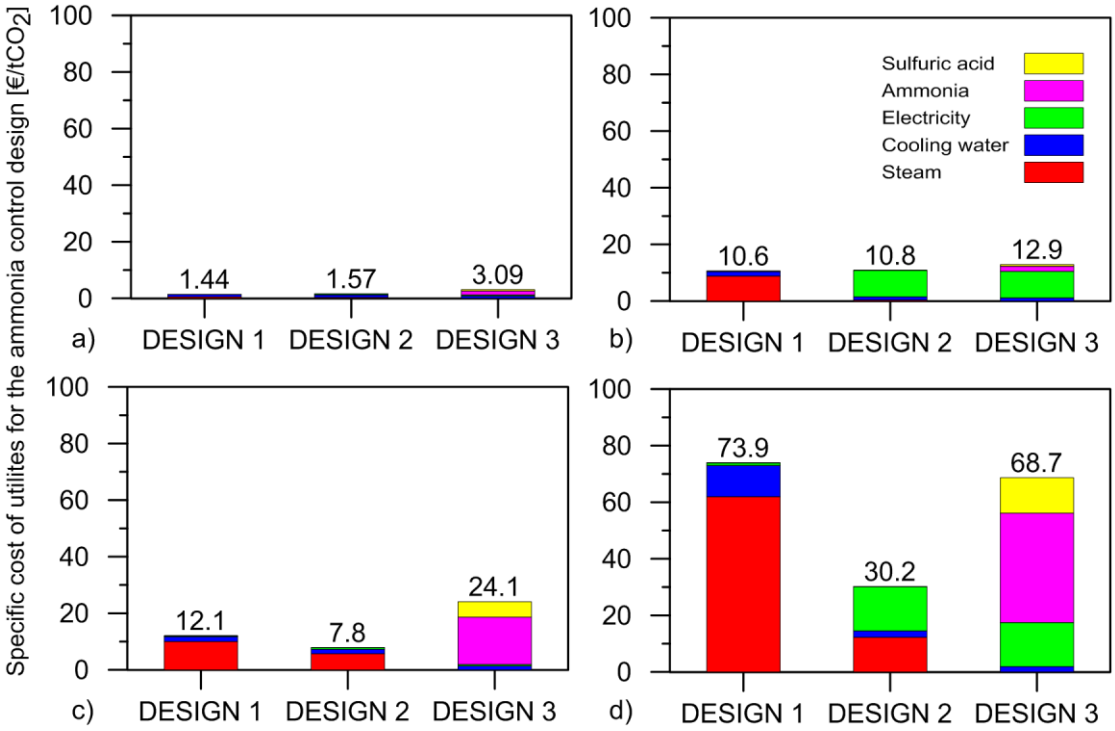

Figure 5.7 The specific utility cost of reducing the ammonia slip to allowable levels for three different designs. The Figure also presents a matrix of the local conditions, cooling water temperature 5°C (a and c) and 25°C (b and d) and flue gas CO_2 concentration 15% (a and b) and 25°C (c and d). Design 1: Staged absorption + Ammonia abatement cycle; Design 2: Staged absorption + Chilled absorption + Ammonia abatement cycle; Design 3, Staged absorption + Chilled absorption + Acid wash. Source: Paper IV.

Water wash

Even if the ammonia slip is minimized in the absorber there is a need to control the emission of ammonia. The most commonly employed measure to accomplish this is to use a water wash column (Unit 5 in Figure 3.1). At the top of the water wash, an almost pure stream of water is distributed over the packing material. The gas stream from the absorber is introduced at the bottom of the water wash. The absorption potential of the water wash is closely related to the pH in the water wash. The pH level determines the extent of the NH_3 dissociation, i.e., the NH_4^+/NH_3 ratio. For the water wash, it is desirable to decrease the pH so as to promote the formation of ammonium, as only free ammonia can evaporate. The presence of other species affects the pH level, and thus the NH_4^+/NH_3 ratio. In this case, CO_2 is present in the water wash, and as CO_2 is a sour gas, the acidity of the liquid will increase, thereby promoting ammonia absorption. Figure 5.8 shows rate-based simulations for a 15 m high water wash under different operating conditions. The figure reveals the water flow rate that is required to ensure exactly 10 ppm ammonia at the water wash outlet. The ammonia slip from the absorber is varied from 1,000 ppm to 100,000 ppm. The amount of water is given as the L/G-ratio (liquid/gas-ratio on mass basis). The gas flow rate from the absorber is set at 240 kg/s. The water wash inlet consists of the given concentrations of ammonia and CO_2, saturated water, and the bulk gas, which is assumed to be nitrogen. To highlight the importance of other influential parameters, the inlet CO_2 concentration is represented by two scenarios (0.5% and 1.5%), and the washing water temperature is represented by two scenarios (10°C and 30°C). In the 30°C scenario, all the simulations can be run up to an ammonia slip of 100,000 ppm. However, the low-temperature scenarios cannot be run up to 100,000 ppm at the fixed state variables (temperature and pressure), due to the problem of condensation. The inlet CO_2 concentrations represent two scenarios in which the original flue gas CO_2 concentration is 5% or 15%, and 90% of the CO_2 is captured in the absorber. As shown in Figure 5.8,

the residual concentration of CO_2 influences how much water is needed. This is due to the fact that some of the CO_2 is absorbed in the water wash and binds some of the ammonia, thereby preventing further evaporation of ammonia. However, the relative level of CO_2 absorption in the water wash is low (0.5% of the total CO_2 inlet), as compared to the amount that is absorbed within the absorber (90%). Even if there is a surplus of ammonia in the absorber off-gas, the absorption of CO_2 is inefficient because the absorption is concomitant along the height of the water wash. The most influential parameter is the temperature of the washing water. This is related to the reduction of the partial pressure by a reduced temperature (see Figure 5.3b). The mass flow of the washing water is highly important, as it is closely related to the heat requirement of the ammonia stripper.

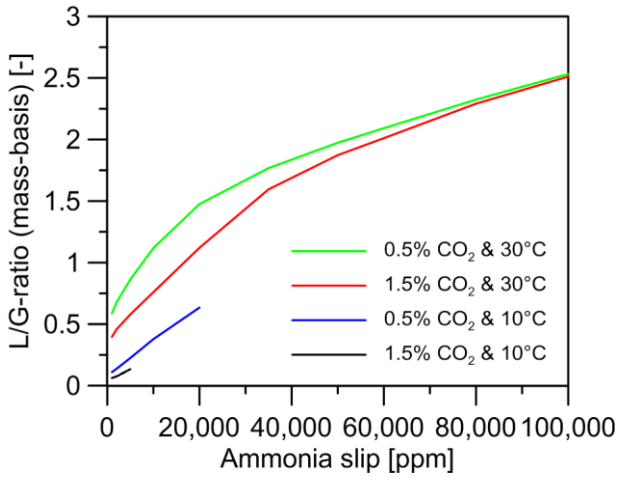

Figure 5.8 Water mass flows required to achieve 10 ppm of ammonia at the water wash gas outlet for varying inlet ammonia concentrations. The water wash is given as the L/G-ratio (liquid/gas-ratio on mass basis). The gas flow rate is 240 kg/s. The figure also shows the results for two different inlet CO_2 concentrations (0.5% and 1.5%) and two different washing water temperatures (10°C and 30°C). Source: Paper IV.

Ammonia abatement cycle

In Figure 5.9, an ammonia abatement cycle (Process C in Figure 3.1) is used to capture and concentrate the ammonia for re-use. Figure 5.9 shows the same operating conditions as in Figure 5.8. However, in this case, the absorber outlet concentration of ammonia is only varied between 0 ppm and 10,000 ppm. The results presented in the figure show the results of a simulation of the whole capture cycle. Figure 5.9 illustrates the specific heat requirement, assuming that 90% of the original CO_2 is captured in the absorber. The heat requirement in Figure 5.9 follows the same trend as that in Figure 5.8. There is a strong correlation between the mass flow rate of the washing water and the heat requirement of the ammonia stripper. This is because a large share of the heat is attributed to the sensible heat required to heat all the water in the ammonia stripper. In Figure 5.9, the heat requirement is divided by the presumed amount of captured CO_2 in the capture cycle. This is in order to relate the two heat demands, which eventually will form the total heat requirement of the process. However, it should be noted that the ammonia stripper is operated at atmospheric pressure, which results in an operating temperature of ~100°C. Thus, steam of lower quality can be used to feed the ammonia stripper compared to the stripper, which is operated at ~155°C. This method is used in Paper V, where stream is extracted at two different pressure levels in the power plant steam cycle. As mentioned in the previous chapter, the heat requirement for the CO_2 capture cycle is minimally 2,500 kJ/kg CO_2: for a more realistic process, it can be up to 3,000 kJ/kg CO_2. Thus, to be competitive with other post-combustion processes (e.g., 3,700 kJ/kg CO_2 for MEA), there is need for the heat of the ammonia abatement cycle to be insignificant. In the absorber simulations performed in this thesis, the ammonia slip from the absorber outlet rarely is less than 2,000 ppm. Even though the residual CO_2 plays an

important part, the major difference is the assumption as to how much CO_2 is already captured, which penalizes the 0.5% CO_2 cases in Figure 5.9. Under the present assumption, it is only in those cases in which there is a low temperature of the washing water (10°C) and a high residual CO_2 (1.5% CO_2) that the heat requirement is sufficiently low (<200 kJ/kg CO_2).

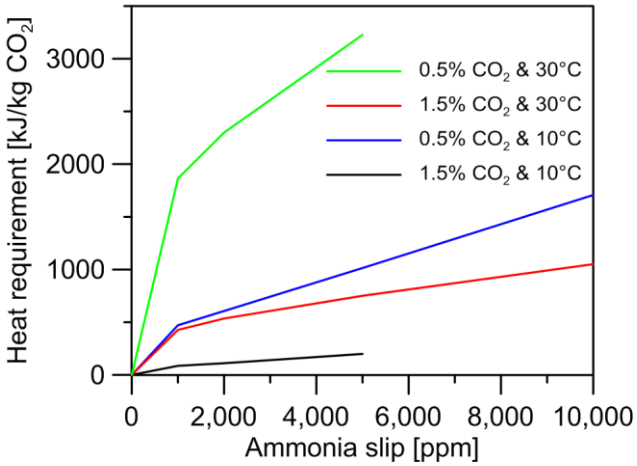

Figure 5.9 Specific heat requirement of the ammonia abatement cycle as a function of ammonia slip. Also shown are the results for two different inlet CO_2 concentrations (0.5% and 1.5%) and two different washing water temperatures (10°C and 30°C). Source: Paper IV.

6. Process Design of the AAP

A full-scale process design for the AAP and a detailed process schematic are presented in this chapter. The design of the AAP is placed in the context of the MEA process. The operating conditions of the AAP are also presented, with special attention focused on the heat requirement for regeneration. Other operational aspects, such as the problem with precipitation in the process, are also discussed. The present chapter includes results from Papers III and V.

6.1. Process description

The schematic of a full-scale, ammonia-based capture process, as proposed in this thesis, is illustrated in Figure 6.1. This includes support systems, such as buffer tanks and maintenance pumps. All the units are numbered according to type. The flue gas stream enters at S1. The present process description assumes a flue gas that is free of contaminants, such as SO_x, NO_x, and fly ash. The flue gas is pressurized in two stages (F1-2), with intermediate cooling in a direct contact water wash (WW1). The majority of the fan work is attributed to F2 due to the lower electricity consumption associated with low-temperature compression. The cooled flue gas enters the absorber setup (A1-2), which is designed according to the description given in Chapter 5.1. The design of the ammonia abatement cycle is described in Paper IV. The process includes five buffer tanks (BT1-4, AT1). Buffer tanks BT1 and BT2 are used for maintenance if the process needs to be evacuated. Thus, there is also a need for pumps for evacuation and refilling. BT3 gathers the condensate from the CO_2 compression system (C1-4, HX11-14) and transports the liquid phase to BT4. All the residual streams are gathered in buffer tank BT4, which serves as a lean solution make-up tank. The concentration of ammonia in the solvent is controlled by an ammonia make-up tank (AT1). The addition of ammonia is based on the 10 ppm slip of ammonia through the stack (S6). The CO_2 compression process is in four stages with intercooling to 20°C. The intercooling heat exchangers (HX11-14) are of the shell-and-tube type. This is due to the high pressure at the hot side and the high pressure difference between the hot side and the cold side. Plate-and-frame heat exchangers have an upper pressure limit of around 20 bar and are sensitive to pressure differences. The two major outlet streams from the process are the stream, which goes to the stack (S6), and the CO_2 stream (S4). The flue gas stream to the stack (S6) meets environmental requirements, and the CO_2 stream (S4) has a purity of 99.5%.

The AAP is more complex than the common MEA-based capture process. One important difference between the ammonia-based and MEA-based processes is the size of the rich/lean heat exchanger. There are three process differences that eventually lead to a larger rich/lean heat exchanger between the ammonia process and the MEA process. The unfavorable aspects from the perspective of the ammonia process is that the absorbent concentration is 14.3 wt% for ammonia (versus 30 wt% for MEA) and the temperature range is about twice as high for ammonia. However, the molecular weight of MEA is about 3.6-times higher than that of ammonia, and the absorbents are expected to operate within the same range of CO_2-loadings.

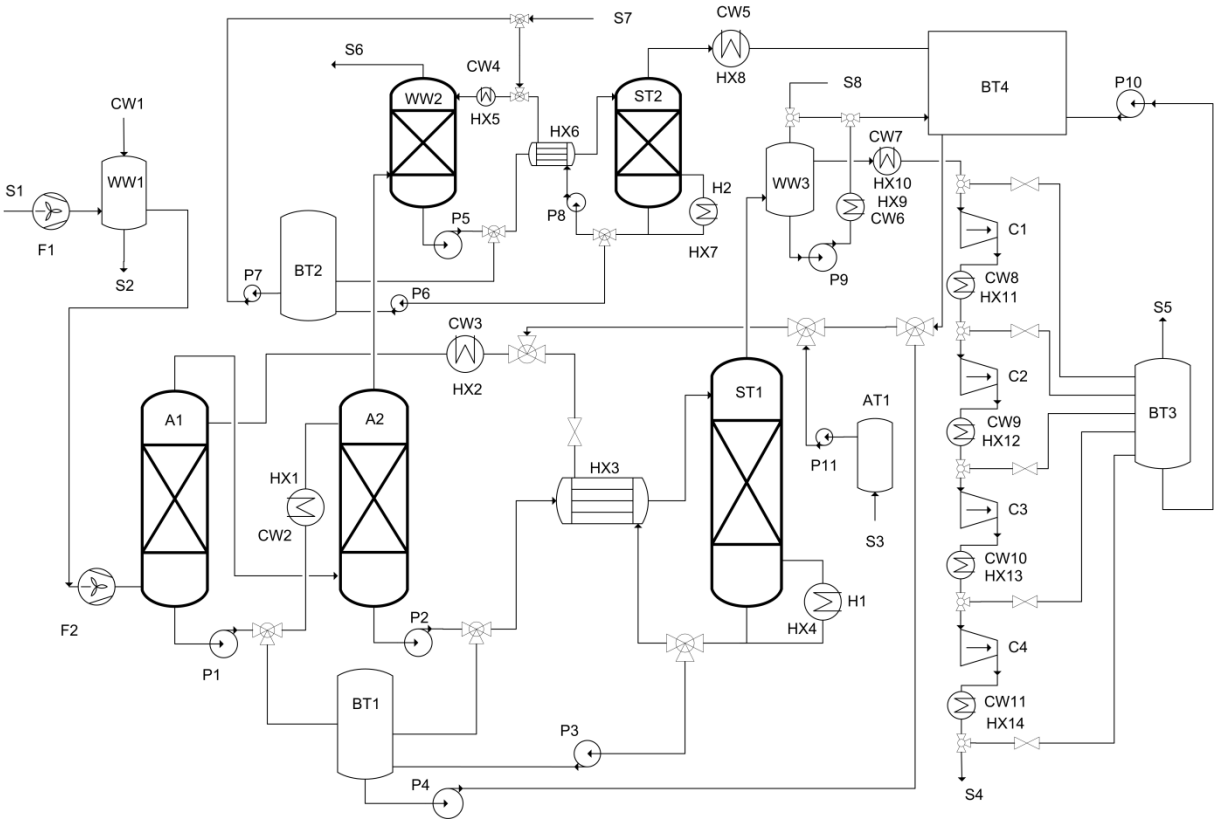

Figure 6.1 Schematic of the process (Paper V), including flue gas pretreatment, CO_2 capture process, CO_2 compression, and ammonia abatement cycle. A, Absorber; ST, stripper; WW, water wash; HX, heat exchanger; P, pump; CW, cooling water; F, fan; C, compressor; BT, buffer tank; S, input/output mass stream; H, heat stream (steam); AT, ammonia tank. Source: Paper V.

An option to reduce the cost of HX3 is presented in Chapter 7. The diameter of the absorber is smaller than that of the corresponding absorber in the MEA process. The volumetric flow rate is reduced by the lower operating temperature. Furthermore, the diameter of the stripper can be lower due to the ten-fold higher pressure in the ammonia process. The upper pressure limit of the stripper is assumed to be limited by the cost of constructing of a large pressurized vessel. However, as mentioned in Chapter 5.2, a high pressure level reduces the ammonia slip.

6.2. Operating conditions of the CO_2 capture cycle

The major components of the CO_2 capture cycle are the absorber, stripper, and the rich/lean heat exchanger (Process B in Figure 3.1). When connected in a closed loop these components form the CO_2 capture cycle. The most important outcomes from the simulations of the CO_2 capture cycle are the capture efficiency, ammonia slip, and heat requirement for regeneration. The simulation approach used in Paper III is entirely equilibrium-based. Thus, the calculated heat requirement should be interpreted as the minimum heat requirement, rather than what the heat requirement would be in an actual capture process. Figure 6.2a presents the heat requirement for regeneration as a function of ammonia concentration and CO_2-loading. The trend change observed at 5% ammonia reflects the start of precipitation. It is important to note that the heat requirement is not enhanced by the presence of solids, not even at high concentrations of ammonia. The gain afforded by the reduced mass flow rate is counteracted by the heat required to dissolve the solids. In Figure 6.2b, the absorber loading is kept constant at 0.5 and the CO_2 capture efficiency is variable (Paper III). For the lowest heat requirement (2200 kJ/kg CO_2), only 50% of the CO_2 is captured.

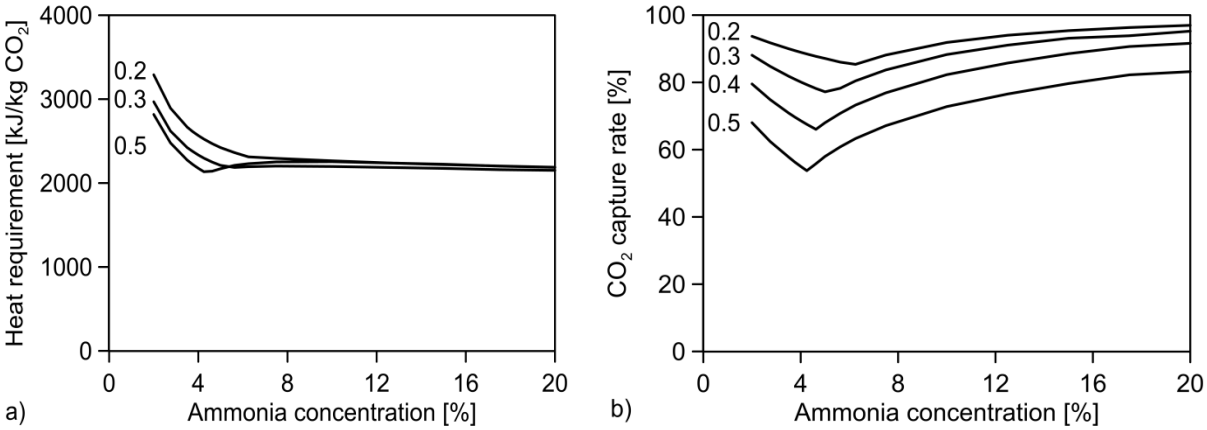

Figure 6.2 The heat requirement for regeneration as a function of ammonia concentration (2%–20%). a) Heat requirements, assuming equilibrium absorption and different lean CO_2-loadings (0.2, 0.3, 0.5). b) CO_2 capture efficiencies for the same simulations. Source: Paper III.

To obtain more accurate predictions of the heat requirement, an actual process rate-based simulation is needed. As stated previously, the heat requirement for regeneration is decreased by a high rich CO_2-loading, and the rate-based simulation limits the rich loading, which will increase the heat requirement. Figure 6.3 shows the heat requirement for ammonia regeneration as a function of ammonia concentration (5%–20%) in the liquid stream in the capture cycle. The simulation represents a rate-based absorber model with a two-absorber setup. In rate-based simulations, no precipitation occurs, even at 20% ammonia. For rate-based simulations, 15% ammonia can be used without with the risk of precipitation. One reason for this is that the absorber loading needs to be much lower for rate-based simulations to achieve the desired capture efficiency. Another reason is that in a non-equilibrium solution, most of the CO_2 will be bound as carbamate, which is not expected to precipitate under these conditions. The modeling procedure depicted in Figure 6.3 differs from Figure 6.2 in that here the capture efficiency is maintained at 90% and the absorber loading is varied. The absorber loading required for 90% capture efficiency is 0.18–0.27. The lean CO_2-loading is set at 0.25. A lean CO_2-loading of up to 0.5, as used in Figure 6.2, would result in negligible absorption. Due to the higher liquid flow rate, the heat requirement will be slightly higher than in Figure 6.2. The heat requirement in the ammonia concentration range of 10.0%–17.5% is 2850–2900 kJ/kg CO_2. There is a clear cost incentive to reduce the heat requirement for regeneration. In Paper V, it is concluded that the cost of steam constitutes 41% of the OPEX of the entire capture process. The left *y*-axis in Figure 6.3 presents the ammonia slip from the absorber. As a result of the staged absorption, the ammonia slip is low (2,000–3,000 ppm) for all ammonia concentrations <17.5%. At ammonia concentrations >17.5%, the ammonia slip rapidly increases to unfeasible concentrations. The reason for this rapid increase is a shift in absorption behavior, which allows CO_2 absorption to occur in the second absorber. The exothermic absorption increases the temperature, and thereby also increases the partial pressure of ammonia. The ammonia concentration is an important parameter, not just for the heat requirement, but also in terms of the slip of ammonia, capture capacity, equipment size, and precipitation behavior. The ammonia concentration will eventually be a trade-off between all of the above-mentioned aspects. Too low a concentration of ammonia will lead to a high heat requirement and high equipment cost. Too high a concentration of ammonia will increase the ammonia slip and increase for the risk of precipitation. The ammonia concentration will also have to be individually determined for each flue gas CO_2 concentration [42].

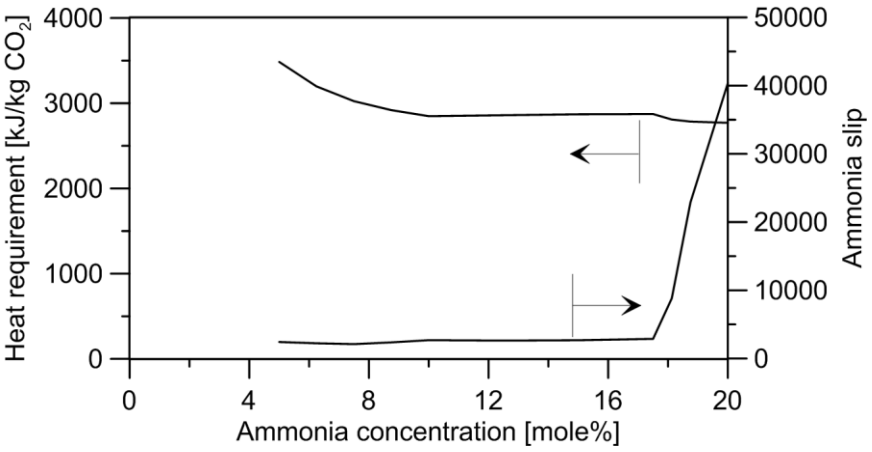

Figure 6.3 Heat requirement for regeneration as a function of ammonia concentration (5%–20%). The figure shows the heat requirement (left *y*-axis) and ammonia slip (right *y*-axis), assuming rate-based absorption. The lean CO_2-loading is 0.25 and the flue gas CO_2 concentration is 15 vol%.

6.3. Precipitation during the process

The risk of precipitation of solid ammonium bicarbonate must be considered for all parts of the process. As mentioned earlier, precipitation is promoted by high CO_2-loadings, high concentrations of ammonia, and low temperatures. All these characteristics are critical in the intercooling (HX1) between absorbers A1 and A2. The temperature and CO_2-loading increase somewhat in A2, which makes it less likely that precipitation will occur in A2 and downstream in HX3. A liquid stream under plausible CO_2-rich stream conditions in the intercooling (CO_2-loading of 0.5, temperature of 10°C. and ammonia concentration of 14.3 wt%) is exactly at the equilibrium precipitation limit of solid ammonium bicarbonate. It is the departure from this equilibrium in the HX1 that prevents precipitation. Thus, any process shut-down may provide enough residence time to cause precipitation in the intercooling. Heat exchangers for which there is the possibility of precipitation are of the shell-and-tube type (HX1-3, HX8-9), while the remainder are of the plate-and-frame type (HX5-6, HX10).

Another part of system where precipitation is likely to occur is the stripper condenser. As shown in Figure 5.6, the slip of ammonia from the stripper can be high, especially at low stripper temperatures. Condensing ammonia in a highly enriched CO_2 atmosphere would most probably lead to precipitation on the condenser walls and eventually, process malfunction. This problem is also highlighted in the work conducted by Yu et al. [80] on the pilot plant operation at the Munmorah power station. Even at a pressure of 20 bar some ammonia remains in the CO_2 stream, and due to the precipitation, it is not likely that a common condenser can be used. This thesis proposes a water wash (WW3) to remove the ammonia and alleviate the problem of precipitation (Paper V). However, a water wash will also absorb some of the CO_2. Due to water-balance issues, the condensate cannot be returned to the stripper. Instead, the CO_2 should be re-introduced into the make-up stream. In the case described in Paper V, the water wash increases the heat requirement from 2,900 kJ/kg to 3,060 kJ/kg CO_2 captured. This effect is therefore not negligible, and becomes increasingly severe if the stripper temperature is decreased. This has some consequences in terms of the application with which this capture process can be integrated. Most industries (e.g., refinery, pulp and paper) have access to excess heat, which can be used for the capture process. However, most of that heat is at temperatures <110°C. As indicated in Figure 5.6, this would result in an energy-consuming process.

7. Process Integration and Cost of the AAP

This chapter evaluates the integration of AAP at the coal-fired NJV power plant. Technical aspects, such as heat integration with the steam cycle in the power plant and the decrease in power plant efficiency, are presented. The technical review forms the basis for the economic estimations of the CAPEX and OPEX of the AAP. A detailed list of the CAPEX and OPEX values is supplied in the appendix to Paper V.

7.1. Integration with CO_2 source

The capture process is connected to the power plant *via* three streams. The flue gases from the power plant (S1) enter the capture process after the existing flue gas cleaning system (NO_x, SO_x, and fly ash). The steam for ammonia regeneration (H1) and the ammonia stripper (H2) is taken from the intermediate pressure part of the steam cycle (IP0, 7.2 bar; and IP1, 1.5 bar). After HX4 and HX7, the condensate is returned to the feed water preheating system at the appropriate temperature. Table 7.1 shows the performance of the power plant when the process described in the previous chapter is integrated with the NJV power plant. The decrease in electric efficiency is estimated as 9.2%, falling from 47.2% to 38.0%. Of these 9.2 percentage points, the loss of steam in the steam cycle accounts for 8.1, while the remainder is attributed to pumping and compression operations. The level of electricity produced by the power plant is reduced by 66.2 MW due to the loss of steam. Both the electricity and cooling water requirements of the power plant are decreased due to the lower mass flow of steam through the low-pressure part of the steam cycle. However, the total electricity and cooling water demands when integrated with the capture process are increased by 38% and 46%, respectively. The cooling water flow rate relative to the cooling requirement is higher for the power plant, due to the lower temperature difference of the cooling water. Most of the cooling requirement is attributed to the absorber intercooling and lean steam cooling. Another large share can be traced to the intercooling of the CO_2 compression. Only 15 MW_{th} of the cooling requirement is needed at temperatures >100°C. Thus, there is little leeway for further optimization. Access to low-temperature cooling water (5°C, yearly average) and a high concentration of CO_2 (15 vol% CO_2 at the absorber inlet) strongly favor the ammonia-based, post-combustion capture process. Under these operating conditions, the ammonia slip is quite low (2,800 ppm), which results in a heat requirement in the ammonia stripper (7.5 MW_{th}). This corresponds to a specific heat requirement of 115 kJ/kg CO_2, which is in line with the bottom line in Figure 5.9. A cooling water temperature of 15°C or 25°C would result in heat requirements for ammonia stripping that would be roughly 2-fold and 6-fold higher, respectively. The consumption of IP0 stream for the ammonia regeneration is 202.3 MW_{th}, which as stated previously corresponds to a specific heat requirement of 3,060 kJ/kg CO_2. Thus, the total heat requirement when the AAP is integrated with the power-plant NJV would be close to 3,200 kJ/kg CO_2.

Table 7.1 Technical performances of the reference plant with and without post-combustion capture. Source: Paper V

	Reference plant without CCS	**Reference plant with CCS**
Fuel input (LHV) (MW_{th})	815.4	815.4
Electricity generation (MW_{th})	408.0	341.8
Power plant auxiliary power (MW_{th})	23.3	22.8
Post-combustion pump operation (MW_{th})		3.87
CO_2 compression (MW_{th})		5.52
Heat requirement (MW_{th})		
- IP0 steam		202.3
- IP1 steam		7.5
Cooling water requirement (MW_{th})		
- Power plant condenser	368	225.5
- Post-combustion		311
Electrical efficiency (%)	47.2	38.0
CO_2 emitted (kg/s)	73.6	7.4
CO_2 captured (kg/s)		66.2

7.2. Cost estimations

The CAPEX is estimated based on all of the units presented in Figure 6.1. Figure 7.1 shows a graphical representation of the CAPEX of each unit, divided into categories. The total installed investment cost is estimated to be 228 M€. The high-cost units include the rich/lean heat exchanger (HX3), the absorber (A1), and the CO_2 compressors (C1-4). It is evident that the cost of the heat exchangers is an important aspect of the total capture cost. The rich/lean heat exchanger (HX3) has by far the highest investment requirement, with 27.7% of the total investment cost. The striped part of HX3 shows the potential cost reduction linked to using plate-and-frame heat exchangers instead of shell-and-tube-type exchangers. The installed cost falls from 63 M€ to 16 M€, which is a significant cost reduction. However, it should be mentioned that the operating conditions of HX3 are on the limits of what is suitable for plate-and-frame heat exchangers, with respect to temperature, pressure, and potential for precipitation. The other cost reduction option has an even higher impact, although it has a lower total investment cost. The option to replace the metallic packing material with a plastic material in absorbers A1 and A2 reduces the investment cost of the column packing material from a total of 11 M€ to 1 M€.

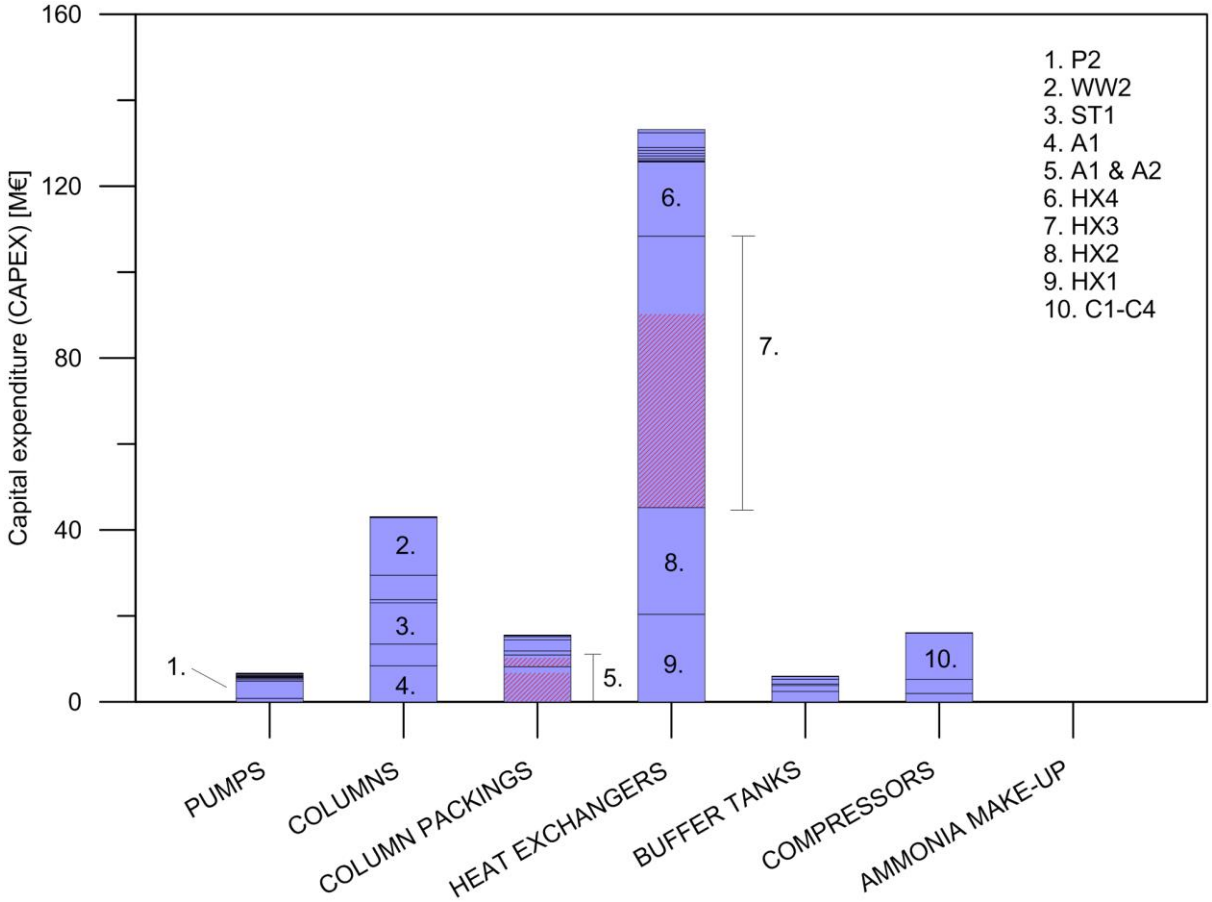

Figure 7.1 Capital expenditures ($€_{2013}$) for all units in the capture process (see Figure 6.1) for the AAP process, as applied to the coal-fired NJV power plant. The units are categorized into types. The numbers shown in the columns denote the major contributors to the total CAPEX. The striped parts of the bars show cost reductions that might be achieved through technical alterations (for column packing materials and heat exchangers). The individual bars are stacked as follows (from bottom to top): Pumps, P1–11; Columns, A1–2, ST1–2, WW1–3; Column packing, A1–2, ST1–2, WW1–3; Heat exchangers, HX1–14; Buffer tanks, BT1–4, AT1; Compressors, F1–2, C1–4; Ammonia make-up, First fill. Source: Paper V.

The OPEX for the capture process is divided into the categories of electricity, steam, cooling water, NH_3 make-up, labor, maintenance, and annualized capital cost. The OPEX values for all the categories are presented in Figure 7.2. The total annual OPEX is estimated as 66.5 M€/year. The capital cost reduction options discussed previously would reduce the total annual OPEX to 59.5 M€/year. As expected, the loss of electricity caused by steam extraction (denoted as 'Steam' in Figure 7.2) is the most influential cost parameter. This is an incentive for research into the identification of absorbents with low heat requirements. The loss of steam is divided into two contributions, one for the stripper (H1) and one for the ammonia stripper (H2). For this application, the cost of reducing the ammonia slip is very low, as only 3.6% of the total heat requirement goes to the ammonia stripper. The reason for the low cost is that the reference power plant has local conditions that allow for low ammonia slip and efficient ammonia removal. Access to low-temperature cooling water (5°C) and the inherently high flue gas CO_2 concentration in coal-fired power plants both favor the control of ammonia slip. The ammonia slip out from the absorber in this application is 2,800 ppm. The ammonia process differs from amine-based capture processes with respect to the cost of make-up. Whereas the amine make-up constitutes 6% of the total utility cost [81], the cost of make-up for ammonia is almost negligible. This is due to the fact that the loss of ammonia is less than 0.03 kg/tCO_2 absorbed. The corresponding value for an amine-based capture process can be more than 100-fold higher. Assuming a load factor of 8,000

h/year for the power plant, the capture process can absorb 1.9 $MtCO_2$ per year. Thus, the specific cost of capture will be 35.0 €/tCO_2 captured.

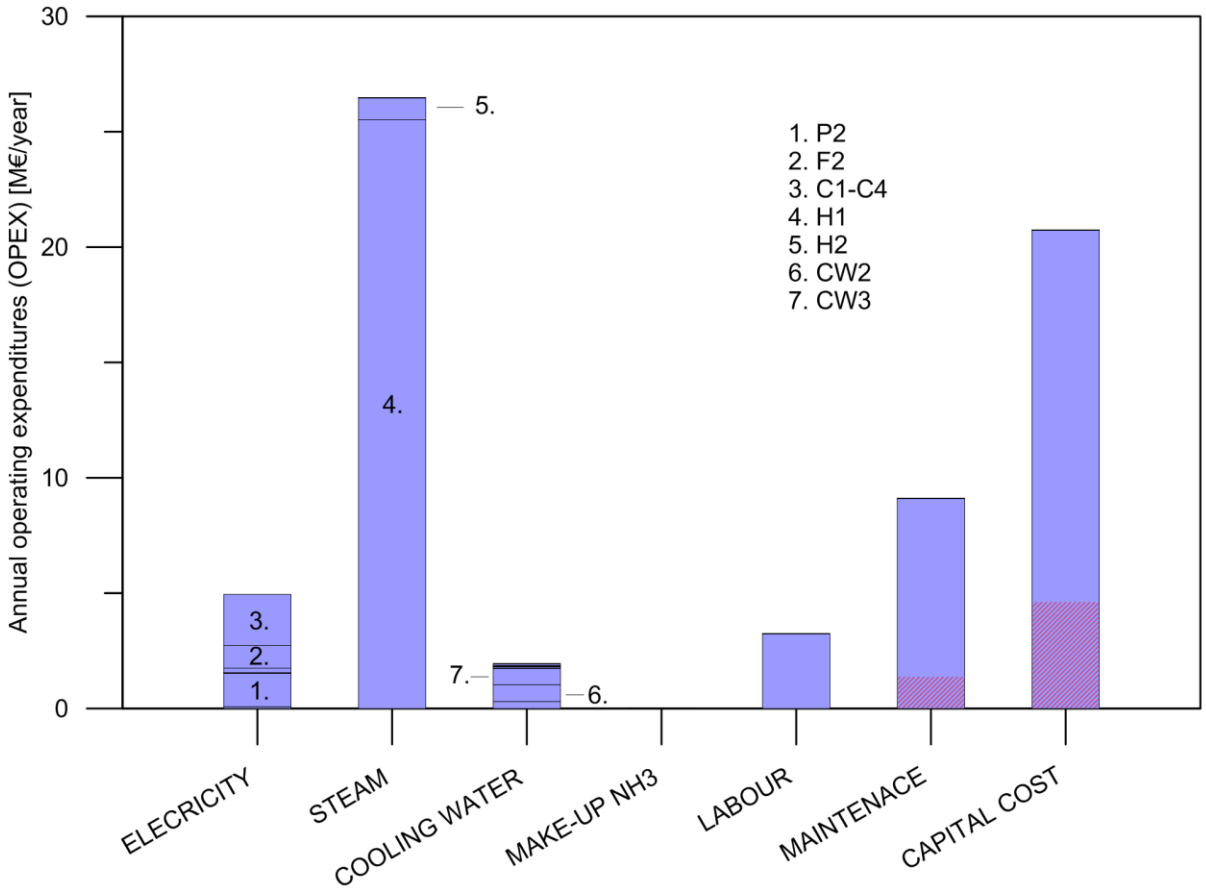

Figure 7.2 Annual operating expenditures ($€_{2013}$) for the AAP process, as applied to the coal-fired NJV power plant, categorized according to the different contributions. The numbers shown in the columns denote the major contributors to the total OPEX. The striped parts of the bars show maintenance and capital cost reductions that might be achieved through process and component design. The individual bars are stacked as follows (from bottom to the top): Electricity, P1–2, P5, P8–11, F1, F2, C1–4; Steam, H1-2; Cooling water, CW1–11; Make-up NH3, S3. Source: Paper V.

8. Discussion

The analyses presented in this thesis offer a comprehensive insight into the performance of ammonia-based, post-combustion capture processes. The process description presented here is the pinnacle of a continuous stream of development since the AAP and the CAP were proposed in 1997 and 2006, respectively. Some of the claims that were made for the initial version of the CAP have proven to be exaggerated, while others remain valid.

Developments in post-combustion capture have often been in relation to the MEA-based process. Even if the MEA process is an established post-combustion capture technique, it does not represent a state-of-the-art process. As presented in Chapter 2.2, there are several candidate absorbents that are superior to MEA. Comparisons with these processes are, however, difficult to conduct because they are less well-known. This is especially true for proprietary solvents, where the performance specifications are very limited. Rochelle and colleagues [13] have proposed that the piperazine-based capture process be used as a new comparative standard next to MEA. As both piperazine and ammonia are second-generation solvents, it is of interest to compare them as well. Table 8.1 offers comparisons of the MEA-, piperazine-, and ammonia-based processes.

The criteria for evaluating absorbent characteristics are presented in Chapter 2.2. The most striking advantages of the ammonia process are its stability and resistance to degradation. Absorbent degradation is a major issue for the amine-based processes, with respect to cost, process design, and environmental effects. There are still major uncertainties associated with amine degradation, which is currently an area of intensive research. However, the cost of MEA replacement (without waste treatment) has proven to be within reasonable limits (less than 5 $\$/tCO_2$). The replacement cost for piperazine is expected to be lower.

The heat requirement for ammonia regeneration is an aspect for which the initial estimations made for the CAP have turned out to be exaggerated. Instead of an initially discussed heat requirement of around 1,000 kJ/kg CO_2, it is more likely that the heat requirement will be close to 3,000 kJ/kg CO_2. This figure does not include the heat required for ammonia stripping, which can vary substantially. The total heat requirement is still expected to be lower than that for the MEA process, although this is not in itself a sufficiently important incentive. The piperazine process is shown in pilot plant operation to have a heat requirement that is similar to that of the ammonia process, i.e., 3,230 kJ/kg CO_2.

The CO_2-loading capacity of ammonia was also initially overestimated. It is shown in this work that is not feasible to operate the process at rich CO_2-loadings >0.5, as the reaction rate is far too low. The initial patent proposed lean and rich loadings in the ranges of 0.25–0.50 and 0.5–1.0, respectively. Based on the present work, it is suggested to operate the absorber at CO_2-loadings of between 0.25 and 0.5, which coincidently, is the same range as for the MEA process. The loading capacity for piperazine is higher, since 2 moles of CO_2 can be absorbed to each mole of piperazine, although the loading range is narrow (0.31–0.41 mol CO_2/2·mol piperazine). Thus, the loading capacities for all three absorbents are similar.

One of the criteria for the absorbent (Table 8.1) that should not be underestimated is the "ease of operation". An end-user values a proven stable operation, even if a more complex option could in theory offer a lower operating cost. In this respect, the MEA process is far more mature than the

second-generation processes. Both the ammonia and piperazine processes are much more complex with respect to process design.

The volatility of ammonia is the major problem associated with the AAP. Although there are technical solutions to control the slip of ammonia, they are expensive. This thesis concludes that the AAP may only be feasible at locations where the conditions allow for a low level of ammonia slip. Crucial to the feasibility of the AAP are the requirements for a source with a relatively high concentration of CO_2 and access to high-quality cooling water. A low level of CO_2 in the flue gas may be solved by reducing the capture efficiency. However, access to large volumes of cooling water at temperatures similar to deep-sea conditions (5°–10°C) is required, which severely limits the number of suitable applications. In comparison to ammonia, the levels of volatility of MEA and piperazine are negligible.

Table 8.1 Comparisons of MEA, ammonia, and piperazine with respect to characteristics relevant for post-combustion capture.

	MEA	**Ammonia**	**Piperazine**
Absorption kinetics	0	-	+
Heat requirement for regeneration	0	+	+
Resistance to degradation	0	+ +	+
CO_2-loading capacity	0	0	-
Corrosiveness	0	+	+
Volatility	0	- -	+
Price	0	+	-
Toxicity	0	0	0
Ease of operation	0	-	-

Key: ++, very advantageous; +, advantageous; 0, similar; -, inferior; --, very inferior.

9. Conclusions

This thesis assesses the potential of ammonia as an absorbent for post-combustion carbon capture. The evaluation is based on experimental, technical, and economic performance analyses. The present work makes contributions to the field in all of these areas. The most important contributions to the field of ammonia-based, post-combustion capture are:

- Experimental equilibrium data for both the gas and liquid phases at temperatures at below 25°C are presented. The new experimental data serve to increase the understanding of the behavior of the NH_3-CO_2-H_2O system in the absorber and may be used to increase the accuracy of thermodynamic modeling. (Paper I)

- Equilibrium-based simulations show that ammonia regeneration for the AAP has a minimum heat requirement of around 2,500 kJ/kg CO_2. This assumes a lean CO_2 loading of 0.25. Rate-based simulations show that departure from the equilibrium state would lead to a heat requirement for the actual process of close to 3,000 kJ/kg CO_2. (Paper III)

- The advantages of using staged absorption are explained in detail. Staged absorption is shown to be crucial for feasible operation, primarily through its ability to confer a significant reduction in ammonia slip. (Paper II)

- For efficient operation, the rich CO_2-loading should not exceed 0.5 in the absorber. Rich CO_2-loadings of >0.5 result in a too high absorber column and lower CO_2-loadings both increase the slip of ammonia and the heat requirement. (Paper II)

- The cost of ammonia-based, post-combustion capture appears to be competitive. The cost of capture at a coastal coal-fired power plant is estimated to be around 35 €/tCO_2. (Paper V)

- Reducing the ammonia slip from the absorber to allowable levels is a crucial design target for the AAP. An ammonia abatement cycle (water wash plus ammonia stripper) in which the ammonia is retained in the process is the ammonia control method that is associated with the lowest cost. Under favorable conditions, such as access to high-quality cooling water (at 5°C) and a relatively high flue gas CO_2 concentration (15%), the utility cost of reducing ammonia slip could be <1.5 €/tCO_2. (Paper IV)

In summary, ammonia-based, post-combustion capture is a viable option for both first- and second-generation absorbents. However, its viability is heavily dependent upon favorable local conditions, and this is related to the penalty of controlling the ammonia slip. Thus, the AAP is suited to niche markets in which conditions or synergetic effects make the process feasible.

10. Suggestions for Future Work

Considering the work and results presented in this thesis, it is clear that there are still major uncertainties associated with ammonia-based, post-combustion capture. With respect to the performance, design, and understanding of the process, the following aspects are proposed as topics for future investigations:

- For successful large-scale commercialization, the ammonia slip problem warrants consideration. Vapor-suppressing additives have been demonstrated to reduce ammonia slip, although the penalty in terms of potentially reduced reactivity remains unclear. The use of residual ammonia for reducing upstream SO_x and NO_x is also a promising alternative that is not fully explored in the present work.

- The slip of ammonia from the stripper also needs further study. This issue is only considered on a quite rudimentary level in this work. As a commonly used condenser cannot be employed due to the problem of precipitation, in the present work, the CO_2 stream is washed with water to remove the residual ammonia. This process is difficult both in terms of modeling and design, due to the high temperature difference and the high concentrations of CO_2. In addition, the water-ammonia mixture absorbs CO_2 with a considerable energy penalty for the process.

- The possibility to use Raman spectroscopy to track the NH_3-CO_2-H_2O system has great potential. The fact that ammonia does not degrade during operation simplifies the spectral analysis, and on-line monitoring of an ammonia capture process with a sufficient time resolution is well within the capabilities of current Raman spectrometers.

- With respect to experimental data, there is a clear lack of new data on the solid precipitation limits and reaction kinetics. Since it is suggested in this thesis to operate close to the precipitation boundary, it is important to know exactly when precipitation starts. Even if the departure from equilibrium hinders precipitation, it is not unlikely that a stop in operation would provide sufficient residence time and cooling to start the precipitation.

- The experimental liquid speciation data produced in Paper I and the comparison with existing data speciation data reveal discrepancies between the experimental data and the model predictions. Even though a large discrepancy was identified for the liquid speciation data, there is some concurrence, especially with respect to the prediction of carbonate.

11. Bibliography

[1] IPCC, *Working Group I Contribution to the IPCC Fifth Assessment Report (AR5), Climate change 2013: The physical science basis*, **2013**.
[2] BP, *BP Statistical Review of World Energy June 2014*, **2014**.
[3] IEA, *World Energy Outlook 2013*, **2013**.
[4] The European Energy Exchange, *Emission Spot Primary Market Auction Report 2014*, **2014**.
[5] Johnsson, F., *Perspectives on CO_2 capture and storage*, Greenhouse Gases: Science and Technology, **2011**, *1*, 119-133.
[6] IPCC, *Summary for Policymakers, Climate Change 2014, Mitigation of Climate Change. Contribution of Working Group III to the Fifth Assessment Report of the Intergovernmental Panel on Climate Change*, **2014**.
[7] Rootzén, J., Johnsson, F., *Exploring the limits for CO_2 emission abatement in the EU power and industry sectors—Awaiting a breakthrough*, Energy Policy, **2013**, *59*, 443-458.
[8] Torp, T. A., Gale, J., *Demonstrating storage of CO_2 in geological reservoirs: The Sleipner and SACS projects*, Energy, **2004**, *29*, 1361-1369.
[9] Bottoms, R. R., *Separating acid gases*, US Patent 1783901, **1930**.
[10] Rochelle, G. T., *Amine scrubbing for CO_2 capture*, Science, **2009**, *325*, 1652-1654.
[11] Kohl, A. L., Nielsen, R. B. *Gas Purification (5th Edition)*, Elsevier, **1997**.
[12] Kamijo, T., Sorimachi, Y., Shimada, D., Miyamoto, O., Endo, T., Nagayasu, H., Mangiaracina, A., *Result of the 60 tpd CO_2 capture pilot plant in European coal power plant with KS-1^{TM} solvent*, Energy Procedia, **2013**, *37*, 813-816.
[13] Rochelle, G., Chen, E., Freeman, S., Van Wagener, D., Xu, Q., Voice, A., *Aqueous piperazine as the new standard for CO_2 capture technology*, Chemical Engineering Journal, **2011**, *171*, 725-733.
[14] Chen, E., Madan, T., Sachde, D., Walters, M. S., Nielsen, P., Rochelle, G. T., *Pilot Plant Results with Piperazine*, Energy Procedia, **2013**, *37*, 1572-1583.
[15] Wang, M., Lawal, A., Stephenson, P., Sidders, J., Ramshaw, C., *Post-combustion CO_2 capture with chemical absorption: A state-of-the-art review*, Chemical Engineering Research and Design, **2011**, *89*, 1609-1624.
[16] Supap, T., Idem, R., Tontiwachwuthikul, P., Saiwan, C., *Kinetics of sulfur dioxide- and oxygen-induced degradation of aqueous monoethanolamine solution during CO_2 absorption from power plant flue gas streams*, International Journal of Greenhouse Gas Control, **2009**, *3*, 133-142.
[17] Fostås, B., Gangstad, A., Nenseter, B., Pedersen, S., Sjøvoll, M., Sørensen, A. L., *Effects of NOx in the flue gas degradation of MEA*, Energy Procedia, **2011**, *4*, 1566-1573.
[18] Arnold, D. S., Barrett, D. A., Isom, R. H., *CO_2 can be produced from flue gas*, Oil & Gas Journal, **1982**, *80*, 130-136.
[19] Wang, S., Hovland, J., Bakke, R., *Anaerobic degradation of carbon capture reclaimer MEA waste*, Water Science and Technology, **2013**, *67*, 2549-2559.
[20] Botheju, D., Glarborg, P., Tokheim, L.-A., *NOx reduction using amine reclaimer wastes (ARW) generated in post combustion CO_2 capture*, International Journal of Greenhouse Gas Control, **2012**, *10*, 33-45.
[21] Rieder, A., Unterberger, S., *EnBW's Post-Combustion Capture Pilot Plant at Heilbronn–Results of the First Year's Testing Programme*, Energy Procedia, **2013**, *37*, 6464-6472.
[22] Bai, H., Yeh, A. C., *Removal of CO_2 greenhouse gas by ammonia scrubbing*, Industrial & Engineering Chemistry Research, **1997**, *36*, 2490-2493.
[23] Gal, E., *Ultra cleaning combustion gas including the removal of CO_2*, World Intellectual Property, 2006022885, **2006**.
[24] Rhudy, R., *Chilled Ammonia Post Combustion CO_2 Capture System - Laboratory and Economic Evaluation Results*, EPRI, Report no 1012797, **2006**.
[25] de Koeijer, G., Enge, Y. O., Thebault, C., Berg, S., Lindland, J., Overå, S. J., *European CO_2 test centre mongstad–Testing, verification and demonstration of post-combustion technologies*, Energy Procedia, **2009**, *1*, 1321-1326.

[26] McLarnon, C. R., Duncan, J. L., *Testing of Ammonia Based CO_2 Capture with Multi-Pollutant Control Technology*, Energy Procedia, **2009**, *1*, 1027-1034.
[27] Powerspan, *Powerspan Announces Results of Independent Assessment of its CO_2 Capture Technology*, http://powerspan.com/press-releases/powerspan-announces-results-of-independent-assessment-of-its-co2-capture-technology/, Accessed August 8, 2014.
[28] MIT, *CCS Project Database*, http://sequestration.mit.edu/tools/projects/map_projects.html, Accessed August 8, 2014.
[29] Darde, V., Thomsen, K., Well, W. J. M. v., Stenby, E. H., *Chilled ammonia process for CO_2 capture*, International Journal of Greenhouse Gas Control, **2009**, *4*, 131-136.
[30] Yu, H., Morgan, S., Allport, A., Cottrell, A., Do, T., McGregor, J., Wardhaugh, L., Feron, P., *Results from trialling aqueous NH_3 based post-combustion capture in a pilot plant at Munmorah power station: Absorption*, Chemical Engineering Research and Design, **2011**, *89*, 1204-1215.
[31] Rhee, C. H., Kim, J. Y., Han, K., Ahn, C. K., Chun, H. D., *Process analysis for ammonia-based CO_2 capture in ironmaking industry*, Energy Procedia, **2011**, *4*, 1486-1493.
[32] Darde, V., Maribo-Mogensen, B., van Well, W. J. M., Stenby, E. H., Thomsen, K., *Process simulation of CO_2 capture with aqueous ammonia using the Extended UNIQUAC model*, International Journal of Greenhouse Gas Control, **2012**, *10*, 74-87.
[33] Valenti, G., Bonalumi, D., Macchi, E., *A parametric investigation of the Chilled Ammonia Process from energy and economic perspectives*, Fuel, **2012**, *101*, 74-83.
[34] Zhang, M., Guo, Y., *Rate based modeling of absorption and regeneration for CO_2 capture by aqueous ammonia solution*, Applied Energy, **2013**, *111*, 142-152.
[35] Valenti, G., Bonalumi, D., Macchi, E., *Energy and exergy analyses for the carbon capture with the Chilled Ammonia Process*, Energy Procedia, **2009**, *1*, 1059-1066.
[36] Dave, N., Do, T., Puxty, G., Rowland, R., Feron, P. H. M., Attalla, M. I., *CO_2 capture by aqueous amines and aqueous ammonia–A Comparison*, Energy Procedia, **2009**, *1*, 1235-1246.
[37] Mathias, P. M., Reddy, S., O'Connell, J. P., *Quantitative evaluation of the chilled-ammonia process for CO_2 capture using thermodynamic analysis and process simulation*, International Journal of Greenhouse Gas Control, **2010**, *4*, 174-179.
[38] Jilvero, H., Normann, F., Andersson, K., Johnsson, F., *Thermal integration and modelling of the chilled ammonia process*, Energy Procedia, **2011**, *4*, 1713-1720.
[39] Valenti, G., Bonalumi, D., Macchi, E., *Modeling of ultra super critical power plants integrated with the chilled ammonia process*, Energy Procedia, **2011**, *4*, 1721-1728.
[40] Kothandarama, A., *Carbon Dioxide Capture by Chemical Absorption: A Solvent Comparison Study*, Dissertation, The Department of Chemical Engineering, Massachusetts Institute of Technology, **2010**.
[41] Versteeg, P., Rubin, E. S., *A technical and economic assessment of ammonia-based post-combustion CO_2 capture at coal-fired power plants*, International Journal of Greenhouse Gas Control, **2011**, *5*, 1596-1605.
[42] Jilvero, H., Mathisen, A., Eldrup, N.-H., Normann, F., Johnsson, F., Müller, G. I., Melaaen, M. C., *Techno-Economic Evaluation of Carbon Capture at an Aluminum Production Plant – Comparison of Post-Combustion Capture using MEA and Ammonia*, To be submitted to The 12th Conference on Greenhouse Gas Control Technologies, **2014**.
[43] Andersson, V., Jilvero, H., Franck, P.-Å., Normann, F., Berntsson, T., *Efficient Utilization of Industrial Excess Heat for Post-combustion CO_2 Capture: An Oil Refinery Sector Case Study*, To be submitted to The 12th Conference on Greenhouse Gas Control Technologies, **2014**.
[44] Linnenberg, S., Darde, V., Oexmann, J., Kather, A., van Well, W. J. M., Thomsen, K., *Evaluating the impact of an ammonia-based post-combustion CO_2 capture process on a steam power plant with different cooling water temperatures*, International Journal of Greenhouse Gas Control, **2012**, *10*, 1-14.
[45] Qin, F., Wang, S., Kim, I., Svendsen, H. F., Chen, C., *Heat of absorption of CO_2 in aqueous ammonia and ammonium carbonate/carbamate solutions*, International Journal of Greenhouse Gas Control, **2011**, *5*, 405-412.
[46] Jänecke, E., *Über das System H_2O, CO_2 und NH_3*, Zeitschrift fuer Elektrochemie, **1929**, *35*, 332-334 + 716-728.

[47] Krop, J., *New approach to simplify the equation for the excess Gibbs free energy of aqueous solutions of electrolytes applied to the modelling of the NH_3–CO_2–H_2O vapour–liquid equilibria*, Fluid Phase Equilibria, **1999**, *163*, 209-229.
[48] Kurz, F., Rumpf, B., Maurer, G., *Vapor-liquid-solid equilibria in the system NH_3-CO_2-H_2O from around 310 to 470 K: New experimental data and modeling*, Fluid Phase Equilibria, **1995**, *104*, 261-275.
[49] Göppert, U., Maurer, G., *Vapor-liquid equilibria in aqueous solutions of ammonia and carbon dioxide at temperatures between 333 and 393 K and pressures up to 7 MPa*, Fluid Phase Equilibria, **1988**, *41*, 153-185.
[50] Pawlikowski, E. M., Newmann, J., Prausnitz, J. M., *Phase equilibria for aqueous solutions of ammonia and carbon dioxide*, Industrial & Engineering Chemistry Process Design and Development, **1982**, *21*, 764-770.
[51] Verbrugge, P., *Vapour-liquid equilibria of the ammonia-carbon dioxide-water system*, Disseration, Delft University, **1973**.
[52] Otsuka, E., Yoshimura, S., Yakabe, M., Inoue, S., *Equilibrium of the NH_3-CO_2-H_2O system*, Kogyo Kagaku Zasshi, **1960**, *62*, 1214-1218.
[53] van Krevelen, D. W., Hoftijzer, P. J., Huntjens, F. J., *Composition and vapour pressures of aqueous solutions of ammonia, carbon dioxide and hydrogen sulphide*, Recueil des Travaux Chimiques des Pays-Bas, **1949**, *68*, 191-216.
[54] Pexton, S., Badger, E. H. M., *The examination of aqueous solutions containing only ammonia and carbon dioxide*, Journal of Society and Chemical Industry, **1938**, *57*, 107-110.
[55] Müller, G., Bender, E., Maurer, G., *Das Dampf-Flüssigkeitsgleichgewicht des ternären Systems Ammoniak-Kohlendioxid-Wasser bei hohen Wassergehalten im Bereich zwischen 373 und 473 Kelvin.*, Berichte der Bunsengesellschaft fuer Physikalische Chemie, **1988**, *92*, 148-160.
[56] Badger, E. H. M., Wilson, D. S., *Vapour pressures of ammonia and carbon dioxide in equilibrium with aqueous. Part VI*, Journal of Society and Chemical Industry, **1947**, *66*, 84-86.
[57] Lichtfers, U., *Spektroskopische Untersuchungen zur Ermittlung von Speziesverteilungen im System Ammonaik-Kohlendioxid-Wasser*, Disseration, University Kaiserslautern **2001**.
[58] Zhao, Q., Wang, S., Qin, F., Chen, C., *Composition Analysis of CO_2−NH_3−H_2O System Based on Raman Spectra*, Industrial & Engineering Chemistry Research, **2011**, *50*, 5316-5325.
[59] Ahn, C. K., Lee, H. W., Chang, Y. S., Han, K., Kim, J. Y., Rhee, C. H., Chun, H. D., Lee, M. W., Park, J. M., *Characterization of ammonia-based CO_2 capture process using ion speciation*, International Journal of Greenhouse Gas Control, **2011**, *5*, 1606-1613.
[60] Holmes, P. E., Naaz, M., Poling, B. E., *Ion concentrations in the CO_2-NH_3-H_2O system from ^{13}C NMR spectroscopy*, Industrial & Engineering Chemistry Research, **1998**, *37*, 3281-3287.
[61] Wen, N., Brooker, M. H., *Ammonium Carbonate, Ammonium Bicarbonate, and Ammonium Carbamate Equilibria: A Raman Study*, The Journal of Physical Chemistry, **1995**, *99*, 359-368.
[62] Mani, F., Peruzzini, M., Stoppioni, P., *CO_2 absorption by NH_3 solutions: speciation of ammonium carbamate, bicarbonate and carbonate by a ^{13}C NMR study*, Green Chemistry, **2006**, *8*, 995-1000.
[63] AspenTech, *Rate-Based Model of the CO_2 Capture Process by NH_3 using Aspen Plus 8.0*, **2013**.
[64] Pinsent, B. R. W., Pearson, L., Roughton, F. J. W., *The kinetics of combination of carbon dioxide with hydroxide ions*, Transactions of the Faraday Society, **1956**, *52*, 1512-1520.
[65] Derks, P. W. J., Versteeg, G. F., *Kinetics of absorption of carbon dioxide in aqueous ammonia solutions*, Energy Procedia, **2009**, *1*, 1139-1146.
[66] Qin, F., Wang, S., Hartono, A., Svendsen, H. F., Chen, C., *Kinetics of CO_2 absorption in aqueous ammonia solution*, International Journal of Greenhouse Gas Control, **2010**, *4*, 729-738.
[67] Darde, V., van Well, W. J. M., Fosboel, P. L., Stenby, E. H., Thomsen, K., *Experimental measurement and modeling of the rate of absorption of carbon dioxide by aqueous ammonia*, International Journal of Greenhouse Gas Control, **2011**, *5*, 1149-1162.
[68] Pinsent, B. R. W., Pearson, L., Roughton, F. J. W., *The kinetics of combination of carbon dioxide with ammonia*, Transactions of the Faraday Society, **1956**, *52*, 1594-1598.
[69] Puxty, G., Rowland, R., Attalla, M., *Comparison of rate of CO_2 absorption into aqueous and monoethanolamine*, Chemical Engineering Science, **2009**, *65*, 915-922.

[70] Versteeg, G. F., van Swaaij, W. P. M., *On the kinetics between CO_2 and alkanolamines both in aqueous and non-aqueous solutions—I. Primary and secondary amines*, Chemical Engineering Science, **1988**, *43*, 573-585.
[71] Darde, V., van Well, W. J. M., Stenby, E. H., Thomsen, K., *Modeling of Carbon Dioxide Absorption by Aqueous Ammonia Solutions Using the Extended UNIQUAC Model*, Industrial & Engineering Chemistry Research, **2010**, *49*, 12663-12674.
[72] Que, H., Chen, C.-C., *Thermodynamic Modeling of the NH_3–CO_2–H_2O System with Electrolyte NRTL Model*, Industrial & Engineering Chemistry Research, **2011**, *50*, 11406-11421.
[73] Thomsen, K., Rasmussen, P., *Modeling of vapor-liquid-solid equilibrium in gas-aqueous electrolyte systems*, Chemical Engineering Science, **1999**, *54*, 1787-1802.
[74] Darde, V., van Well, W. J. M., Stenby, E. H., Thomsen, K., *CO_2 capture using aqueous ammonia: kinetic study and process simulation*, Energy Procedia, **2011**, *4*, 1443-1450.
[75] Valenti, G., Bonalumi, D., Fosbøl, P., Macchi, E., Thomsen, K., Gatti, D., *Alternative Layouts for the Carbon Capture with the Chilled Ammonia Process*, Energy Procedia, **2013**, *37*, 2076-2083.
[76] Chen, C.-C., Britt, H. I., Boston, J. F., Evans, L. B., *Local composition model for excess Gibbs energy of electrolyte systems. Part I: single solvent, single completely dissociated electrolyte systems.* , AIChE J., **1982**, *28*, 588–596.
[77] Qi, G., Wang, S., Yu, H., Wardhaugh, L., Feron, P., Chen, C., *Development of a rate-based model for CO_2 absorption using aqueous NH_3 in a packed column*, International Journal of Greenhouse Gas Control, **2013**, *17*, 450-461.
[78] Onda, K., Takeuchi, H., Okumoto, Y., *Mass transfer coefficients between gas and liquid phases in packed columns*, Journal of Chemical Engineering of Japan, **1968**, *1*, 56-62.
[79] European Commission, *Quarterly Report on European Electricity Markets, Volume 6, Issue 2, Second quarter 2013*, **2013**.
[80] Yu, H., Qi, G., Wang, S., Morgan, S., Allport, A., Cottrell, A., Do, T., McGregor, J., Wardhaugh, L., Feron, P., *Results from trialling aqueous ammonia-based post-combustion capture in a pilot plant at Munmorah Power Station: Gas purity and solid precipitation in the stripper*, International Journal of Greenhouse Gas Control, **2012**, *10*, 15-25.
[81] Mores, P., Rodríguez, N., Scenna, N., Mussati, S., *CO_2 capture in power plants: Minimization of the investment and operating cost of the post-combustion process using MEA aqueous solution*, International Journal of Greenhouse Gas Control, **2012**, *10*, 148-163.